FONDAZIONE BRUNO KESSLER

ECT* EUROPEAN CENTRE FOR THEORETICAL STUDIES IN NUCLEAR PHYSICS AND RELATED AREAS

SIDIS off unpolarized protons at COMPASS

Andrea Moretti

on behalf of the COMPASS Collaboration

Opportunities with JLab energy and luminosity upgrade – ECT (Trento) 26-30/09/2022*

Introduction

Semi-Inclusive Deep Inelastic Scattering (SIDIS) is a powerful tool to access the rich and complex structure of the nucleon.

Depending on the nucleon polarization, several (TMD)-PDFs can be accessed

In this talk: focus on the SIDIS off unpolarized nucleons

Nucleon \ Quark	**U** unpolarized	**L** longitudinally polarized	**T** transversely polarized
U unpolarized	$f_1^q(x,k_T^2)$ **number density**		$h_1^{\perp q}(x,k_T^2)$ **Boer-Mulders**
L longitudinally polarized		$g_1^q(x,k_T^2)$ **helicity**	$h_{1L}^{\perp q}(x,k_T^2)$ **Kotzinian-Mulders worm-gear L**
T transversely polarized	$f_{1\perp}^q(x,k_T^2)$ **Sivers**	$g_{1T}^{\perp q}(x,k_T^2)$ **Kotzinian-Mulders worm-gear T**	$h_1^q(x,k_T^2)$ **transversity** $h_{1T}^{\perp q}(x,k_T^2)$ **Pretzelosity**

Cross section for unpolarized SIDIS

In SIDIS, a high energy lepton scatters off a nucleon target and at least one hadron is observed in the final state.

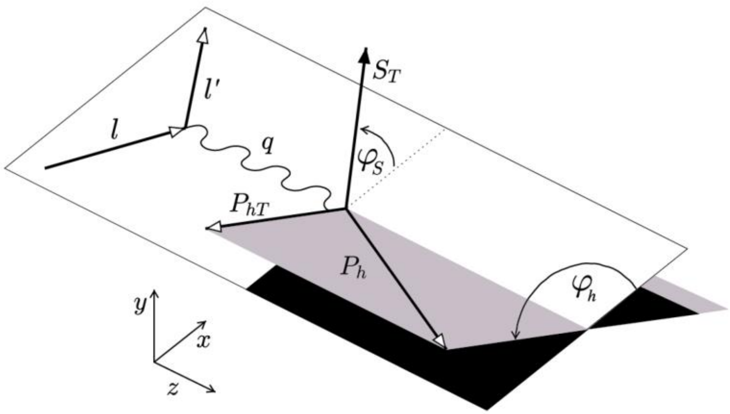

The Gamma Nucleon System (GNS)

For an unpolarized nucleon target and in the one-photon exchange approximation **the fully-differential cross-section** reads:

$$\frac{d^5\sigma}{dx\,dy\,dz\,d\varphi_h dP_T^2} = \frac{2\pi\alpha^2}{xyQ^2}\frac{y^2}{2(1-\varepsilon)}\left(1+\frac{\gamma^2}{2x}\right)$$

$$\cdot\left(F_{UU,T} + \varepsilon F_{UU,L} + \sqrt{2\varepsilon(1+\varepsilon)}F_{UU}^{\cos\varphi_h}\cos\varphi_h + \varepsilon F_{UU}^{\cos 2\varphi_h}\cos 2\varphi_h + \lambda_l\sqrt{2\varepsilon(1-\varepsilon)}F_{LU}^{\sin\varphi_h}\sin\varphi_h\right)$$

Bacchetta et al., *JHEP* 02 (2007) 093

- x is the Bjorken variable
- Q^2 the photon virtuality
- $\gamma = \frac{2Mx}{Q}$ (small in COMPASS kinematics)
- $y = 1 - \frac{E_{\ell'}}{E_\ell}$ the inelasticity with $E_{\ell(')}$ the energy of the incoming (scattered) lepton in the target rest frame
- $\varepsilon(y) = \frac{1-y-\frac{1}{4}\gamma^2 y^2}{1-y+\frac{1}{2}y^2+\frac{1}{4}\gamma^2 y^2}$

- λ_l is the beam polarization.
- z is the fraction of photon energy carried by the hadron
- φ_h its azimuthal angle in the Gamma Nucleon System
- P_T its transverse momentum w.r.t. the photon

Cross section for unpolarized SIDIS

In SIDIS, a high energy lepton scatters off a nucleon target and at least one hadron is observed in the final state.

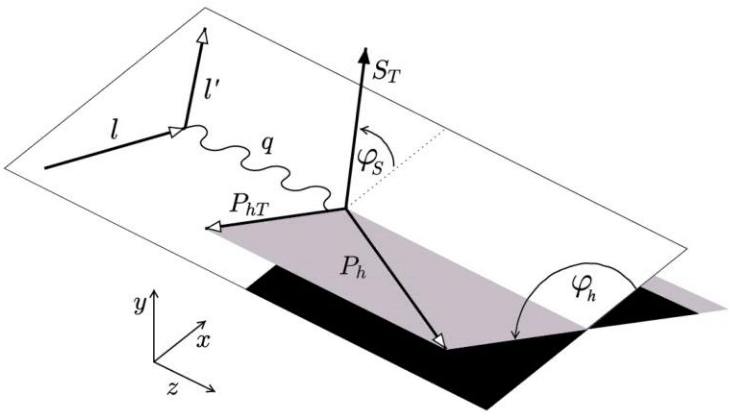

The Gamma Nucleon System (GNS)

For an unpolarized nucleon target and in the one-photon exchange approximation **the fully-differential cross-section** reads:

Bacchetta et al., *JHEP* 02 (2007) 093

$$\frac{d^5\sigma}{dx\,dy\,dz\,d\varphi_h dP_T^2} = \frac{2\pi\alpha^2}{xyQ^2}\frac{y^2}{2(1-\varepsilon)}\left(1+\frac{\gamma^2}{2x}\right)$$

$$\cdot\left(F_{UU,T} + \varepsilon F_{UU,L} + \sqrt{2\varepsilon(1+\varepsilon)}F_{UU}^{\cos\varphi_h}\cos\varphi_h + \varepsilon F_{UU}^{\cos 2\varphi_h}\cos 2\varphi_h + \lambda_l\sqrt{2\varepsilon(1-\varepsilon)}F_{LU}^{\sin\varphi_h}\sin\varphi_h\right)$$

The structure functions $F_{XY[,Z]}^{[f(\varphi_h)]}$ can be written at high Q^2 in terms of

- TMD Parton Distributions Functions (PDFs)
- TMD Fragmentation Functions (FFs).

Unpolarized structure functions

Unpolarized SIDIS → access to the **number density TMD** and to the **Boer-Mulders TMD** $h_1^{\perp}$

Quark \ Nucleon	**U** unpolarized	**L** longitudinally polarized	**T** transversely polarized
U unpolarized	$f_1^q(x,k_T^2)$ number density		$h_1^{\perp q}(x,k_T^2)$ Boer-Mulders

Boer-Mulders function $h_1^{\perp}$ couples to the **Collins FF $H_1^{\perp}$**: fragmentation of a transversely polarized quarks into hadron

The correlation between $\boldsymbol{k_T}$ and $\boldsymbol{s_T}$ *generates* a neat quark transverse polarization

Up to order $1/Q$ (i.e. at twist-3) in Wandzura-Wilczek approximation *:

$$F_{UU,T} = \mathcal{C}[f_1 D_1]$$

Cahn effect *Boer-Mulders term*

$$F_{UU}^{\cos\varphi_h} = \frac{2M}{Q}\mathcal{C}\left[-\frac{(\hat{h}\cdot\vec{k}_T)}{M}f_1 D_1 - \frac{(\hat{h}\cdot\vec{p}_\perp)k_T^2}{zM^2M_h}h_1^{\perp}H_1^{\perp} + \cdots\right]$$

$$F_{UU}^{\cos 2\varphi_h} = \mathcal{C}\left[-\frac{2(\hat{h}\cdot\vec{k}_T)(\hat{h}\cdot\vec{p}_\perp) - \vec{k}_T\cdot\vec{p}_\perp}{zM\,M_h}h_1^{\perp}H_1^{\perp}\right]$$

Boer-Mulders term

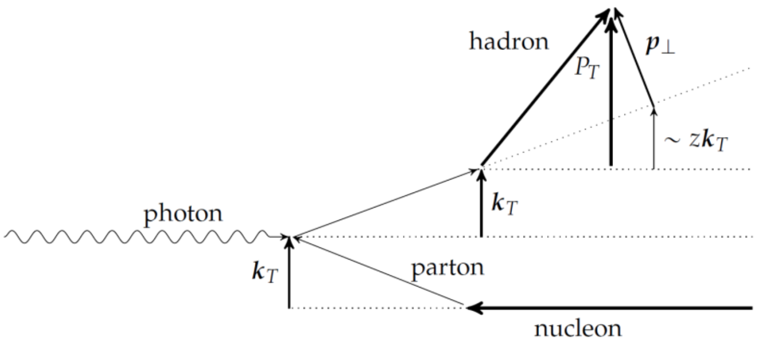

where $\mathcal{C}[wfD]$ is the convolution over the unobservable transverse momenta:

$$\mathcal{C}[wfD] = x\sum_a e_a^2\int d^2\vec{k}_T\int d^2\vec{p}_\perp\delta^2(\vec{P}_T - \vec{k}_T - \vec{p}_\perp)w(\vec{k}_T,\vec{p}_\perp)f^a(x,\vec{k}_T)D^a(z,\vec{p}_\perp)$$

$$\hat{h} = \vec{P}_T\,/\,|\vec{P}_T|$$

* possible further contributions at high z from the *Berger-Brodsky* mechanism
Brandenburg et al., *Phys.Lett.B* 347 (1995) 413-418

Unpolarized structure functions

Gaussian Ansatz → the TMD PDFs and FFs factorize as:

$$f_1^q(x,k_T^2) = f_1^q(x)\,\frac{e^{-\frac{k_T^2}{\langle k_{T,q}^2\rangle}}}{\pi\langle k_{T,q}^2\rangle} \qquad D_1^{h/q}(z,p_\perp^2) = D_1^{h/q}(z)\,\frac{e^{-\frac{p_\perp^2}{\langle p_{\perp,h/q}^2\rangle}}}{\pi\langle p_{\perp,h/q}^2\rangle}$$

from which, assuming flavour independence, it follows that e.g.

$$F_{UU,T} = x\,\sum_q e_q^2 f_1^q(x) D_1^{h/q}(z)\,\frac{e^{-\frac{P_T^2}{\langle P_T^2\rangle}}}{\pi\langle P_T^2\rangle}$$

→ P_T^2 distributions

$$F_{UU\,|\,Cahn}^{\cos\varphi_h} = -\frac{2zP_T\langle k_T^2\rangle}{Q\langle P_T^2\rangle} F_{UU,T}$$

$$F_{UU\,|\,BM}^{\cos\varphi_h} = -\frac{2P_T\langle k_T^2\rangle\langle p_\perp^2\rangle}{zQMM_h\langle P_T^2\rangle^3}\left(\langle p_\perp^2\rangle\langle P_T^2\rangle + z^2\langle k_T^2\rangle(P_T^2-\langle P_T^2\rangle)\right)\frac{\sum_q x h_1^{\perp q}(x) H_1^\perp(z)}{\sum_q x f_1^q(x) D_1(z)}\,F_{UU,T}$$

$$F_{UU|BM}^{\cos 2\varphi_h} = \frac{P_T^2\langle k_T^2\rangle\langle p_\perp^2\rangle}{MM_h\langle P_T^2\rangle^2}\frac{\sum_q x h_1^{\perp q}(x) H_1^\perp(z)}{\sum_q x f_1^q(x) D_1(z)}\,F_{UU,T}$$

→ Azimuthal asymmetries

Both sets of observables measured in COMPASS with an unpolarized proton target after well known measurements on deuteron

EPJC 73 (2013) 2531
PRD 97(2018) 032006
NPB 886 (2014) 1046
NPB 956 (2020) 115039

The COMPASS experiment

COMPASS contribution to the understanding of the nucleon structure

- spin asymmetries with transverse and longitudinal spin polarization
  important results on the extraction of transversity and Sivers functions
- SIDIS with unpolarized target
  azimuthal asymmetries and P_T^2-distributions on deuteron

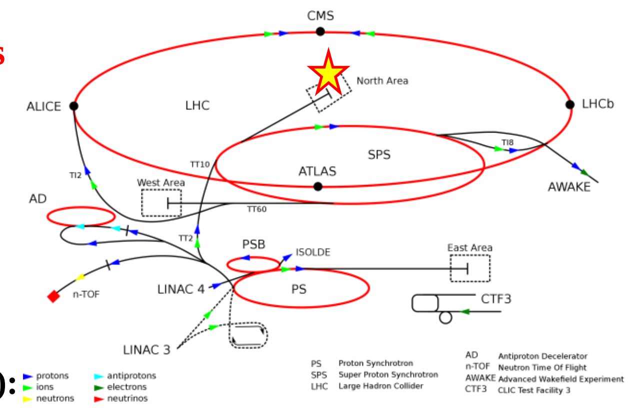

COMPASS (COmmon Muon Proton Apparatus for Structure and Spectroscopy):

- 24 institutions from 13 countries (about 220 physicists)
- a fixed target experiment
- located in the CERN North Area, along the SPS M2 beamline

Broad research program:

- SIDIS with μ beam, with (un)polarized deuteron or proton target.
- Hadron spectroscopy with hadron beams and nuclear targets
- Drell-Yan measurement with π^- beam with polarized target
- Deeply Virtual Compton Scattering (DVCS)
- …

A multipurpose apparatus:

- Two-stage spectrometer, about 330 detector planes
- μ identification, RICH, calorimetry

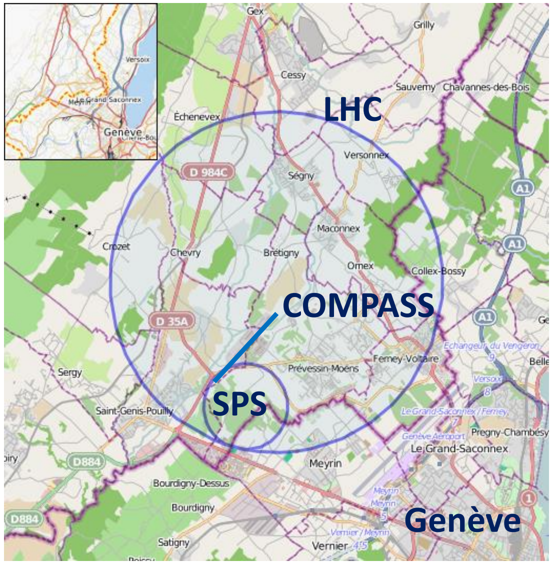

The COMPASS location at CERN

The 2016 COMPASS run

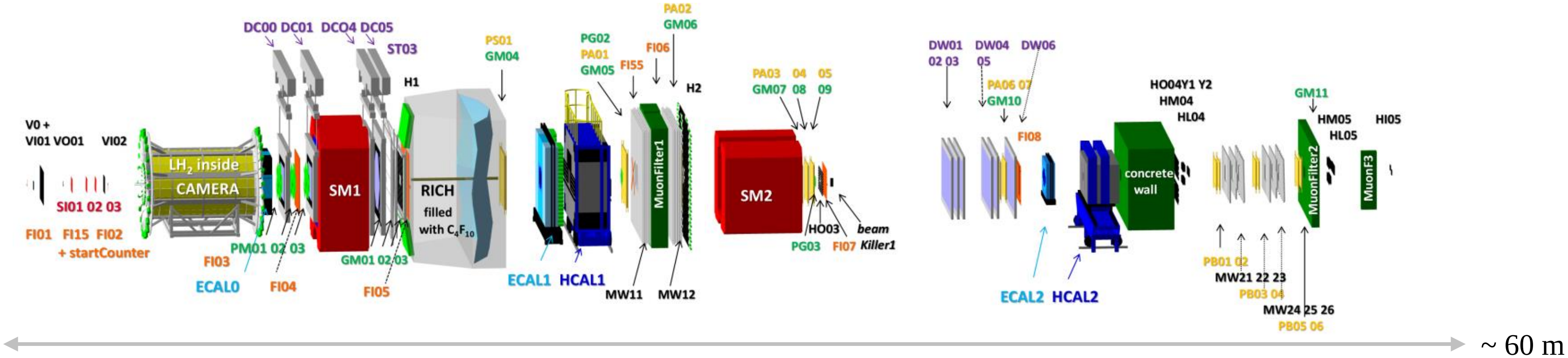

The 2016 COMPASS experimental setup

In 2016 (and 2017) the data-taking was dedicated to the measurement of Deeply Virtual Compton Scattering (DVCS).

In parallel, new SIDIS data have been collected in COMPASS, with:

- 160 GeV/c μ beam (μ^+ and μ^- with balanced statistics)
- Unpolarized, 2.5 m long **liquid hydrogen target**

Part of the data has been analyzed → ~ 6.5 million hadrons

Here: a selection of the results

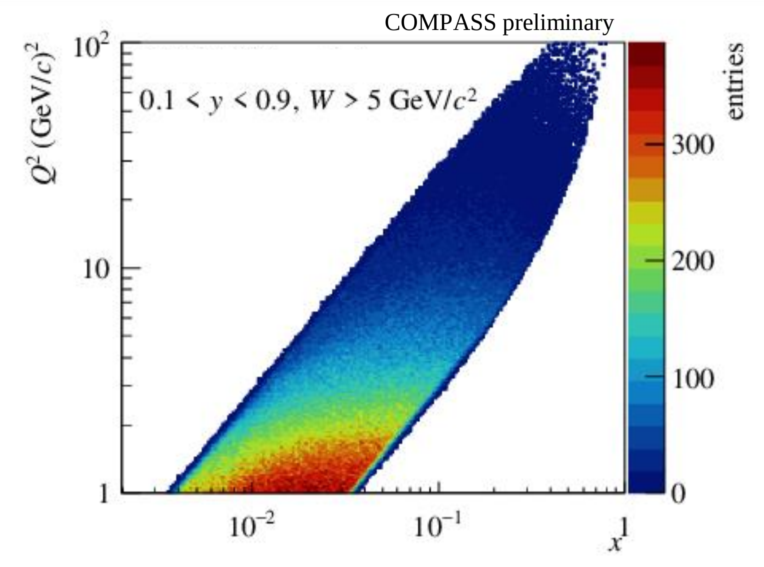

The $x - Q^2$ coverage

Event and hadron selection

Events and hadron selection – standard

$Q^2 > 1\ (\text{GeV}/c)^2$

$W\ > 5\ \text{GeV}/c^2$

$0.003 < x < 0.130$

$0.2 < y < 0.9$

$\theta_\gamma < 60\ \text{mrad}$

$z > 0.1$

$P_T > 0.1\ \text{GeV}/c$

Non-negligible fraction of the selected hadrons:

produced in the decay of diffractively-produced vector mesons

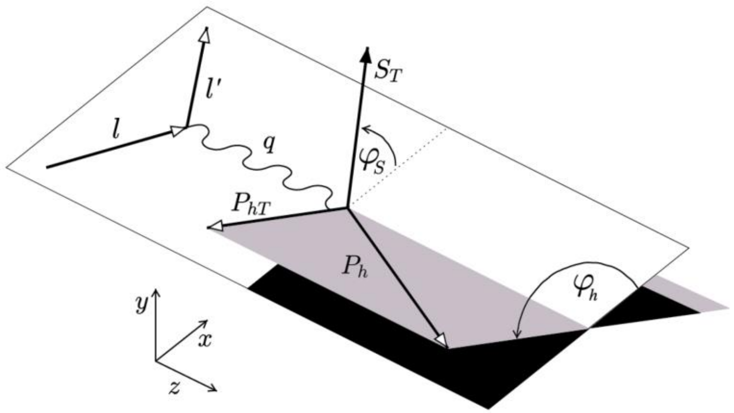

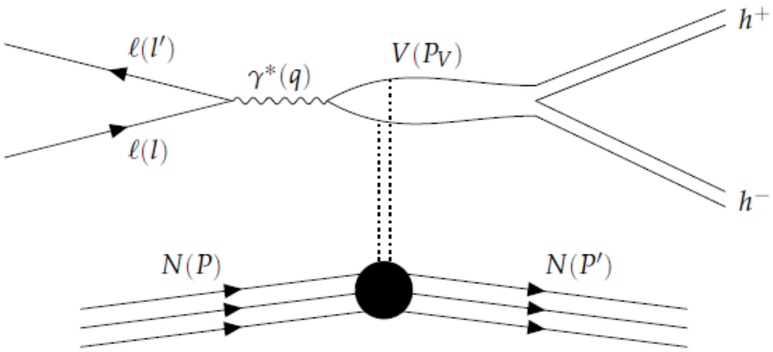

Contribution from exclusive hadrons

Hadrons from the decay of exclusive diffractive vector mesons *(exclusive hadrons)*, very interesting per se, constitute a relevant source of background for the SIDIS measurement.

The two most important channels: $\rho^0 \to \pi^+\pi^-$ *and* $\phi \to K^+K^-$

- Well visible in the data at vanishing missing energy

$$E_{miss} = \frac{M_X^2 - M_p^2}{2M_p}$$

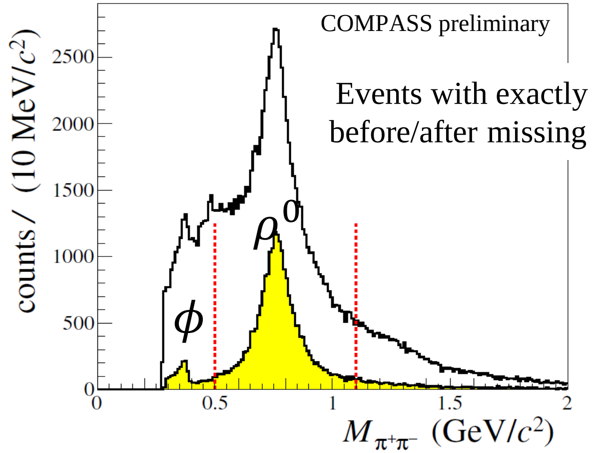

Events with exactly 2 hadrons before/after missing energy cut

Impact on the azimuthal asymmetries measured on a deuteron target: COMPASS, *Nucl.Phys.B* 956 (2020) 115039

Contribution from exclusive hadrons

Hadrons from the decay of exclusive diffractive vector mesons *(exclusive hadrons)*, very interesting per se, constitute a relevant source of background for the SIDIS measurement.

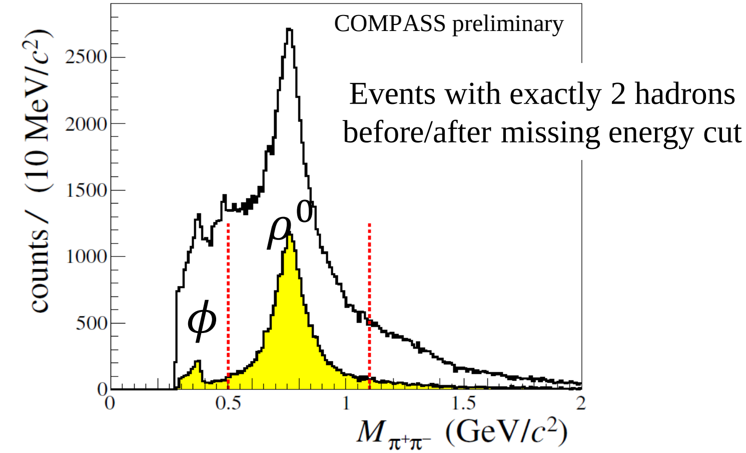

The two most important channels: $\rho^0 \to \pi^+\pi^-$ *and* $\phi \to K^+K^-$

- Well visible in the data at vanishing missing energy

$$E_{miss} = \frac{M_X^2 - M_p^2}{2M_p}$$

- Strong modulations in the azimuthal angle
- Contamination as high as 30% at high z

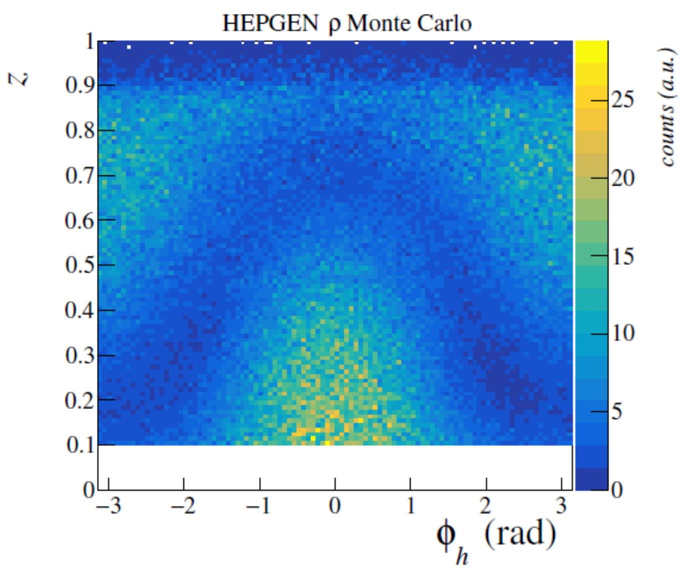

$\phi_h - z$ correlation for exclusive hadrons

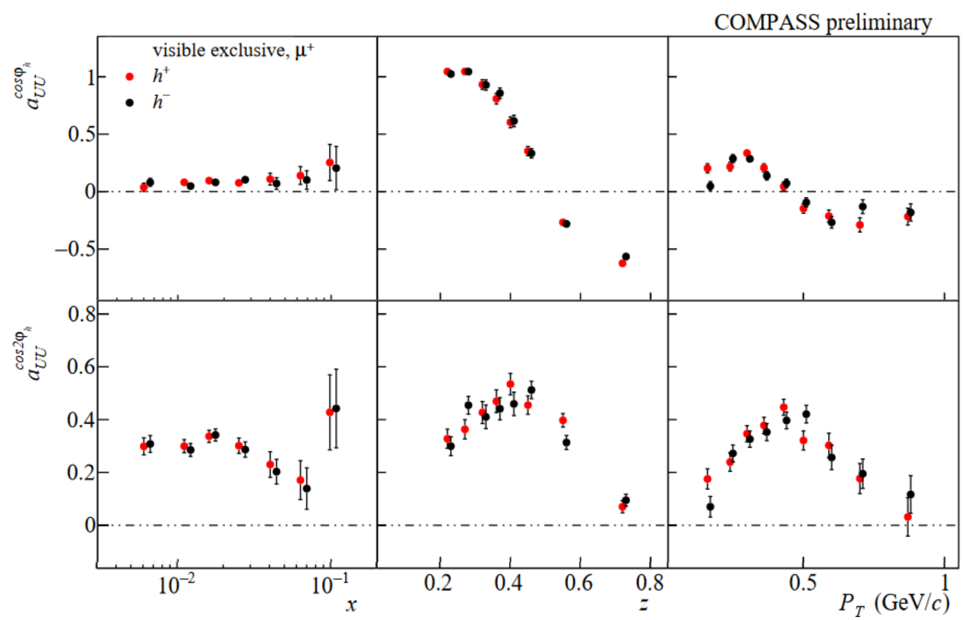

Impact on the azimuthal asymmetries measured on a deuteron target: COMPASS, *Nucl.Phys.B* 956 (2020) 115039

Contribution from exclusive hadrons

Estimated exclusive hadrons contaminations in the data:
~80% is fully reconstructed

- The fully reconstructed exclusive events are discarded in the analysis
  - The partially reconstructed is estimated from Monte Carlo

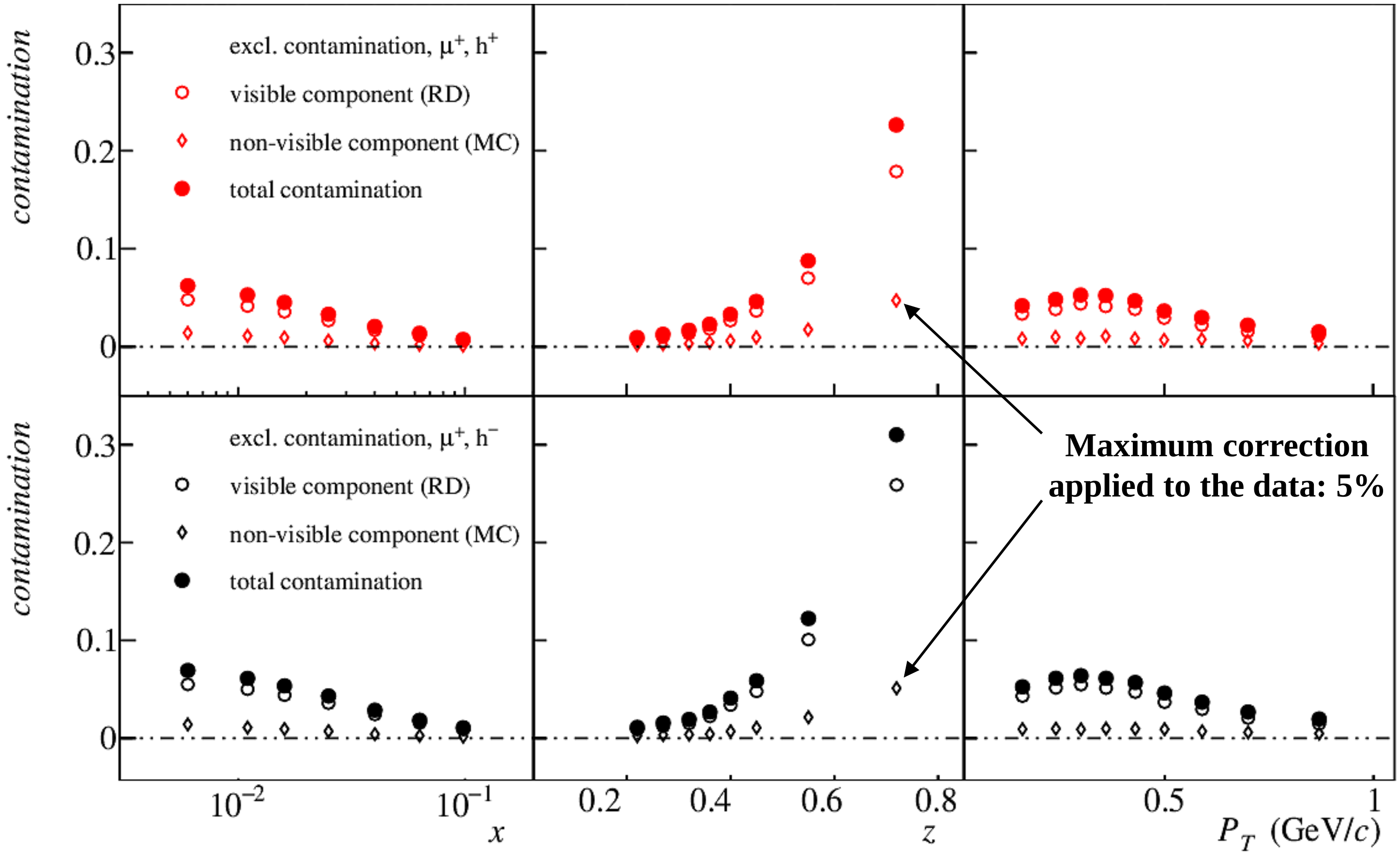

Maximum correction applied to the data: 5%

Contribution from exclusive hadrons

Estimated exclusive hadrons contaminations in the data:
~80% is fully reconstructed

- The fully reconstructed exclusive events are discarded in the analysis
  - The partially reconstructed is estimated from Monte Carlo

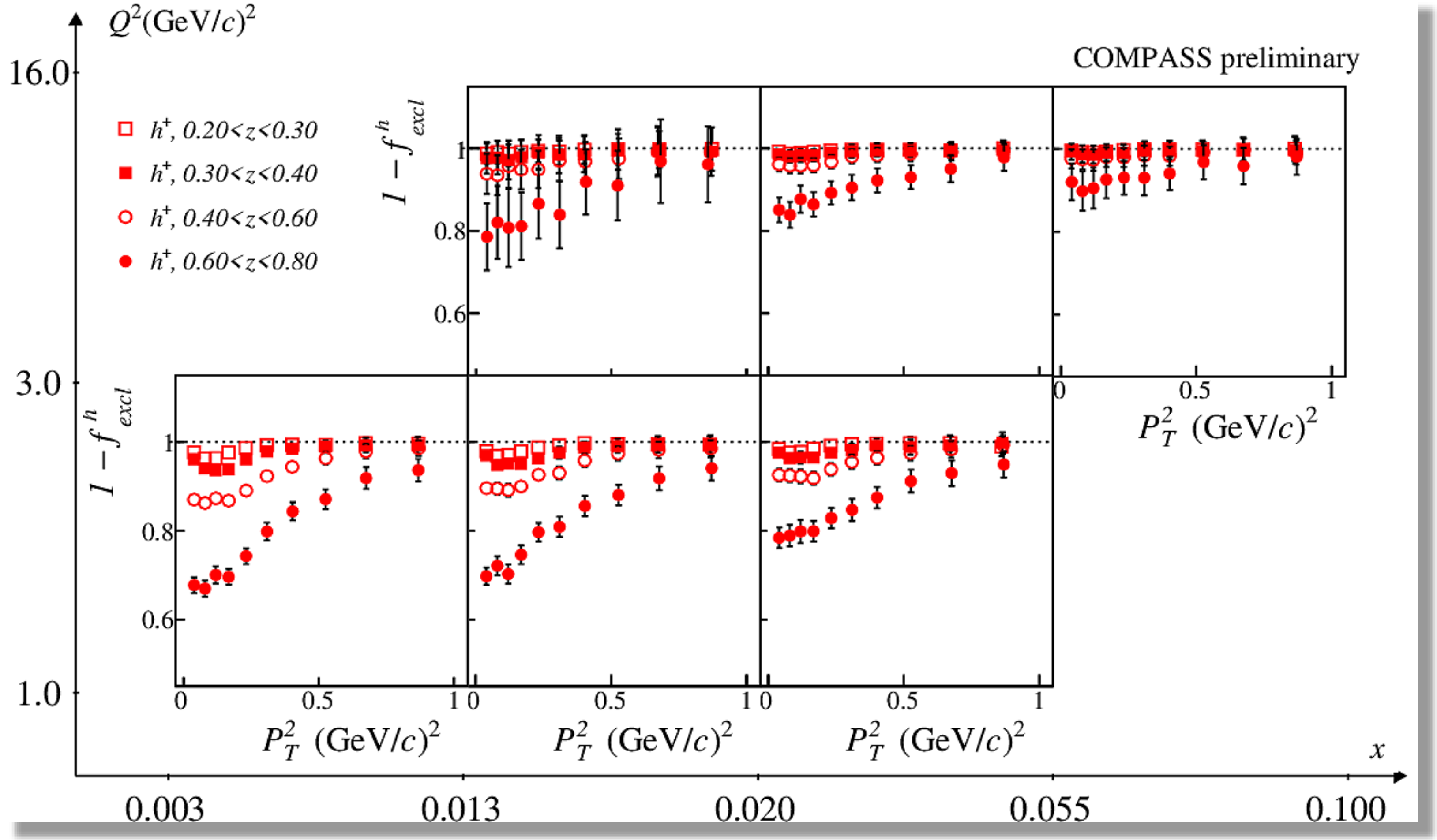

Transverse momentum distributions

Transverse-momentum distributions
- give relevant information on k_T and $p_\perp$
- are interesting for the TMD evolution studies:
  a lot of theoretical work to reproduce the experimental distributions over a large energy range

In gaussian approximation, at small values of P_T, the number of hadrons is expected to follow:

$$\frac{d^2N^h(x,Q^2;z,P_T^2)}{dz\,dP_T^2} \propto \exp\left(-\frac{P_T^2}{\langle P_T^2\rangle}\right)$$

$$\langle P_T^2\rangle = z^2\langle k_T^2\rangle + \langle p_\perp^2\rangle$$

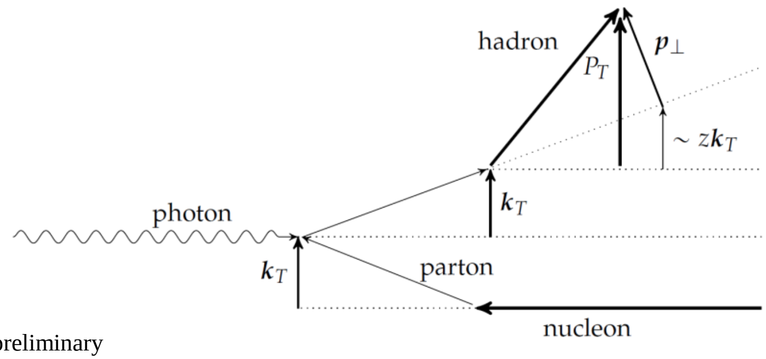

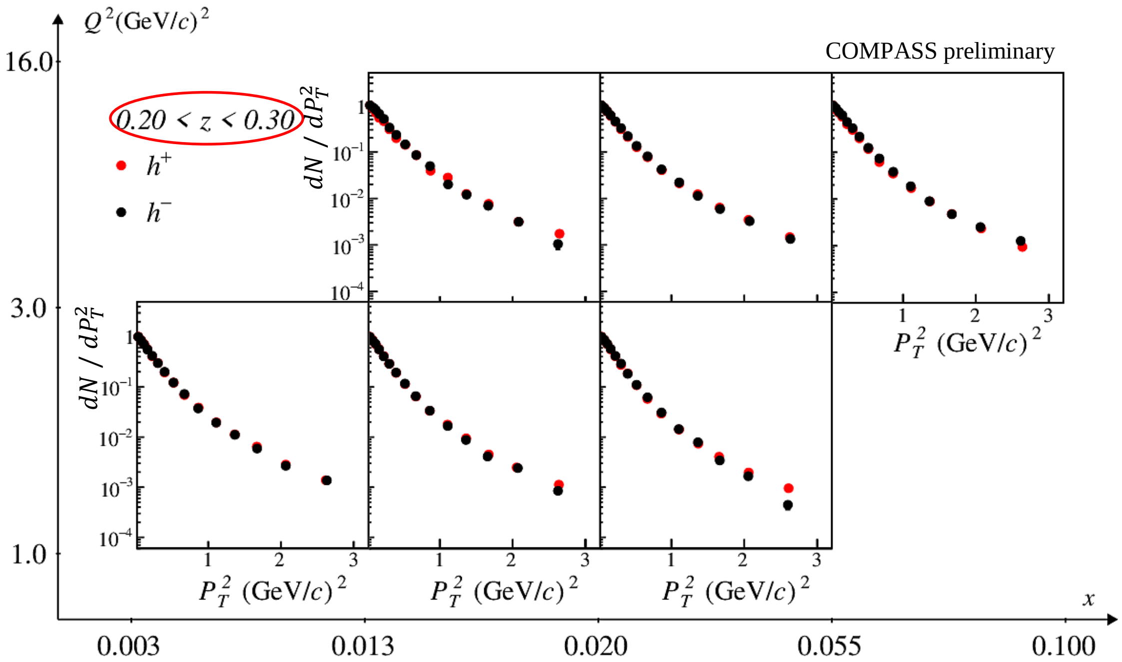

- **Normalization: first P_T^2 bin.**
- Different normalization for each bin and charge
- Two different slopes for P_T above / below 1 GeV/c
- Perturbative effects expected to contribute more there
- Likely not sufficient to explain the high- P_T trend

e.g. Gonzales-Hernandez et al., *Phys.Rev.D* 98 (2018) 11, 114005

Transverse momentum distributions

The error bars correspond to the statistical uncertainty only. $\sigma_{syst} \sim 0.3\, \sigma_{stat}$

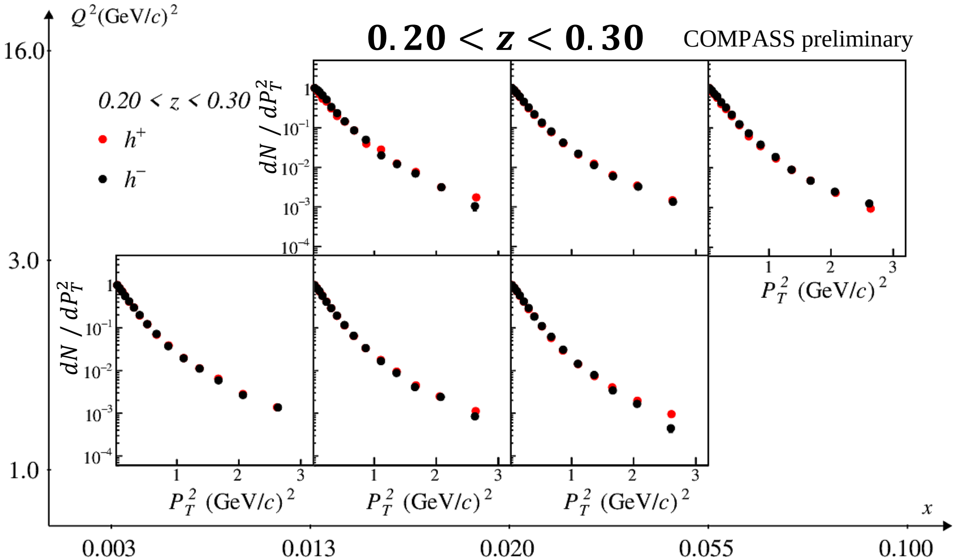

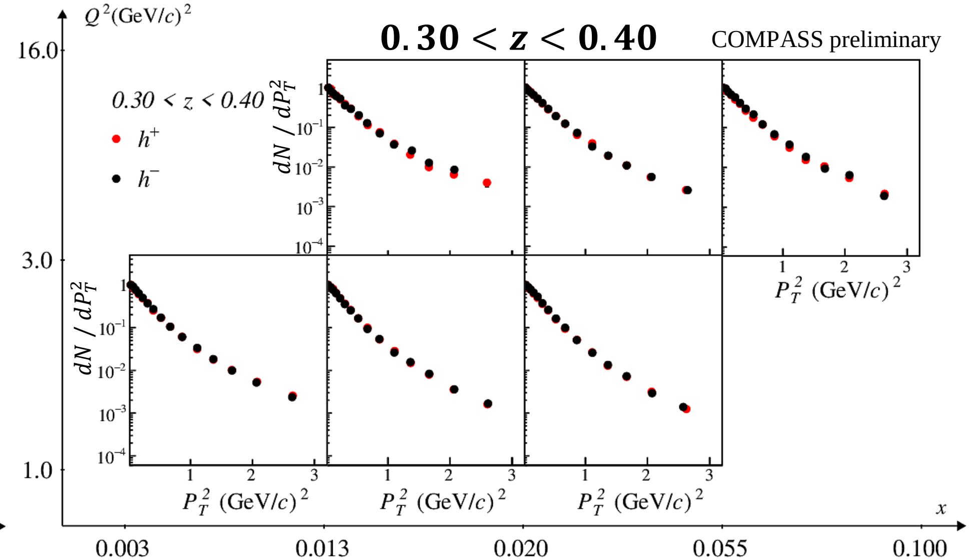

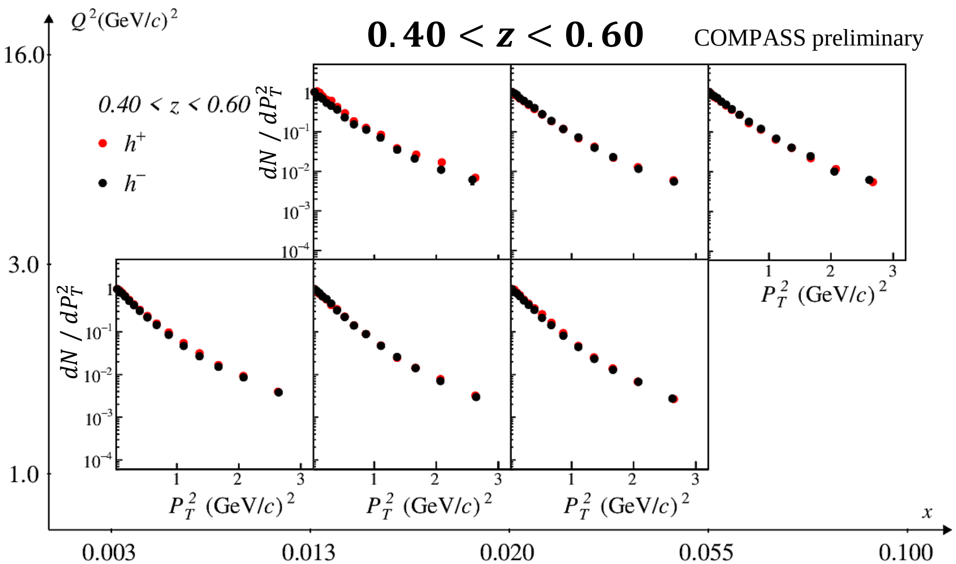

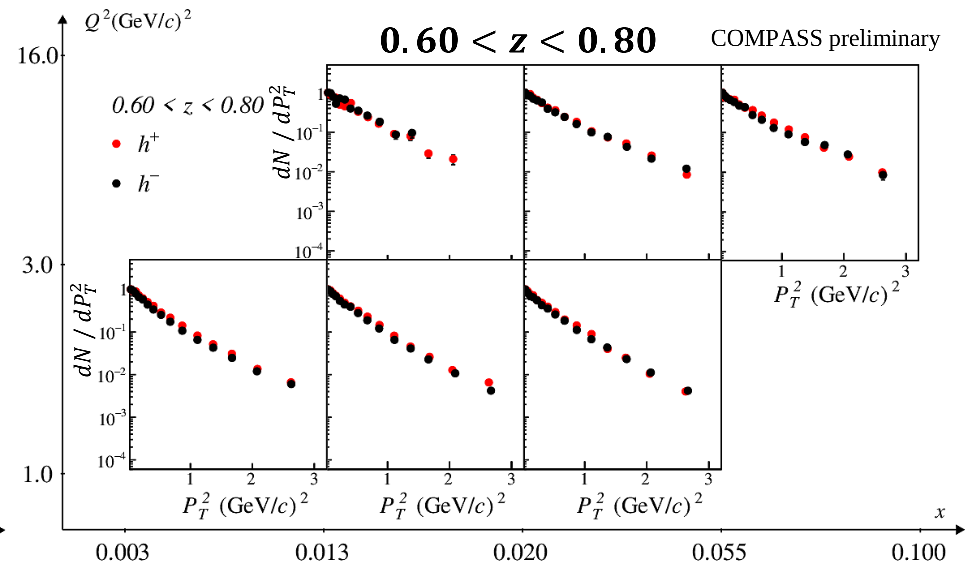

Fit of the P_T^2 - distributions

P_T^2 − distributions fitted with three different functions:

- a single-exponential up to 1 GeV/c : $f(x) = \alpha \exp\left(-\frac{x}{\beta}\right) \Longrightarrow \langle P_T^2 \rangle = \beta$
- a double-exponential up to 3 GeV/c : $g(x) = A \exp\left(-\frac{x}{a}\right) + B \exp\left(-\frac{x}{b}\right) \Longrightarrow \langle P_T^2 \rangle = \frac{Aa^2+Bb^2}{Aa+Bb}$
- a Tsallis-like power law up to 3 GeV/c : $h(x) = c_0(1+c_1 x)^{-c_2} \Longrightarrow \langle P_T^2 \rangle = \frac{1}{c_1(c_2-2)}$

Very similar results

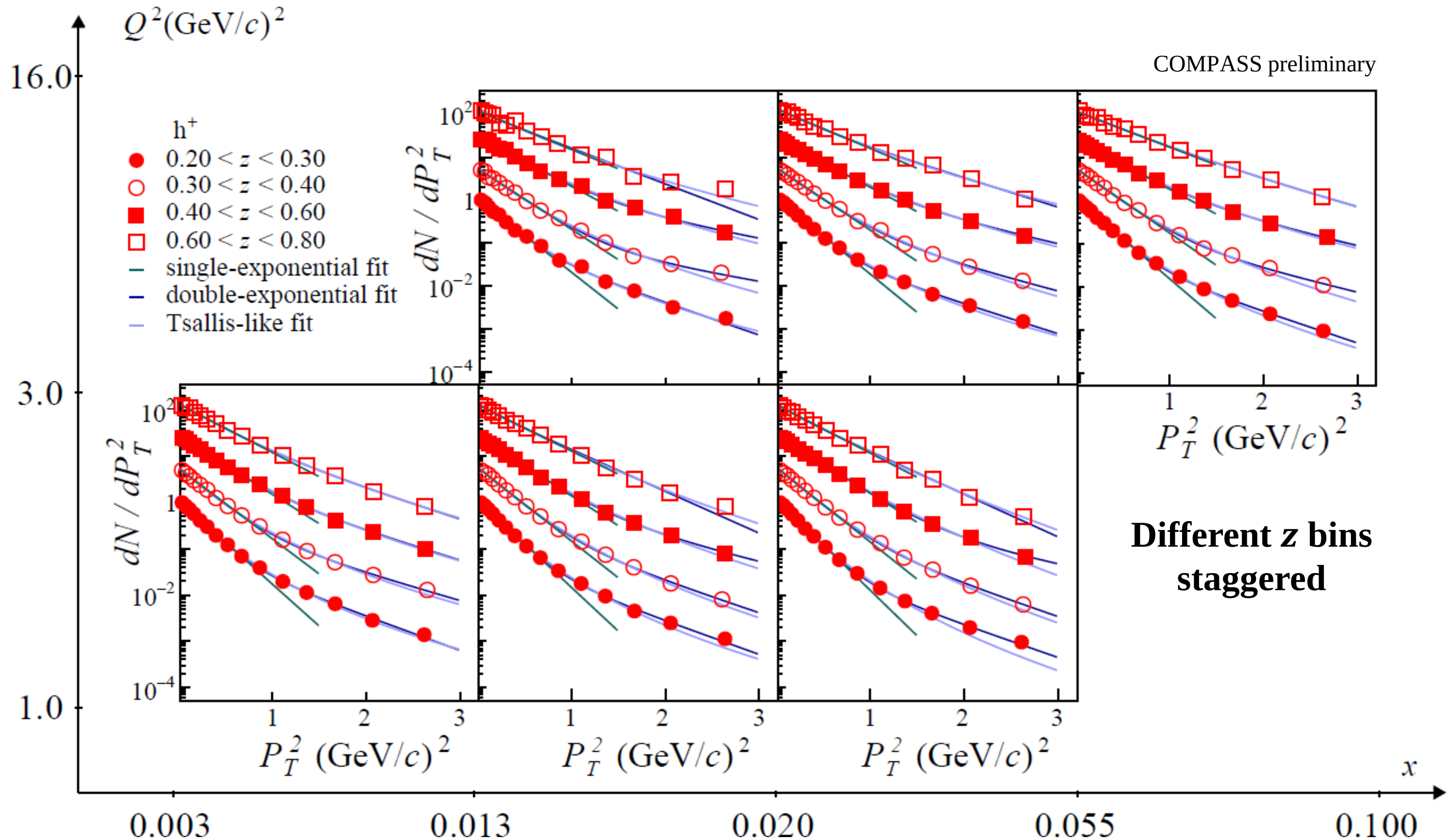

Different z bins staggered

Fit of the P_T^2 - distributions

Leading Order expectation: $\langle P_T^2 \rangle = z^2 \langle k_T^2 \rangle + \langle p_\perp^2 \rangle$
Deviation from linearity: already there with the deuteron multiplicities / distributions

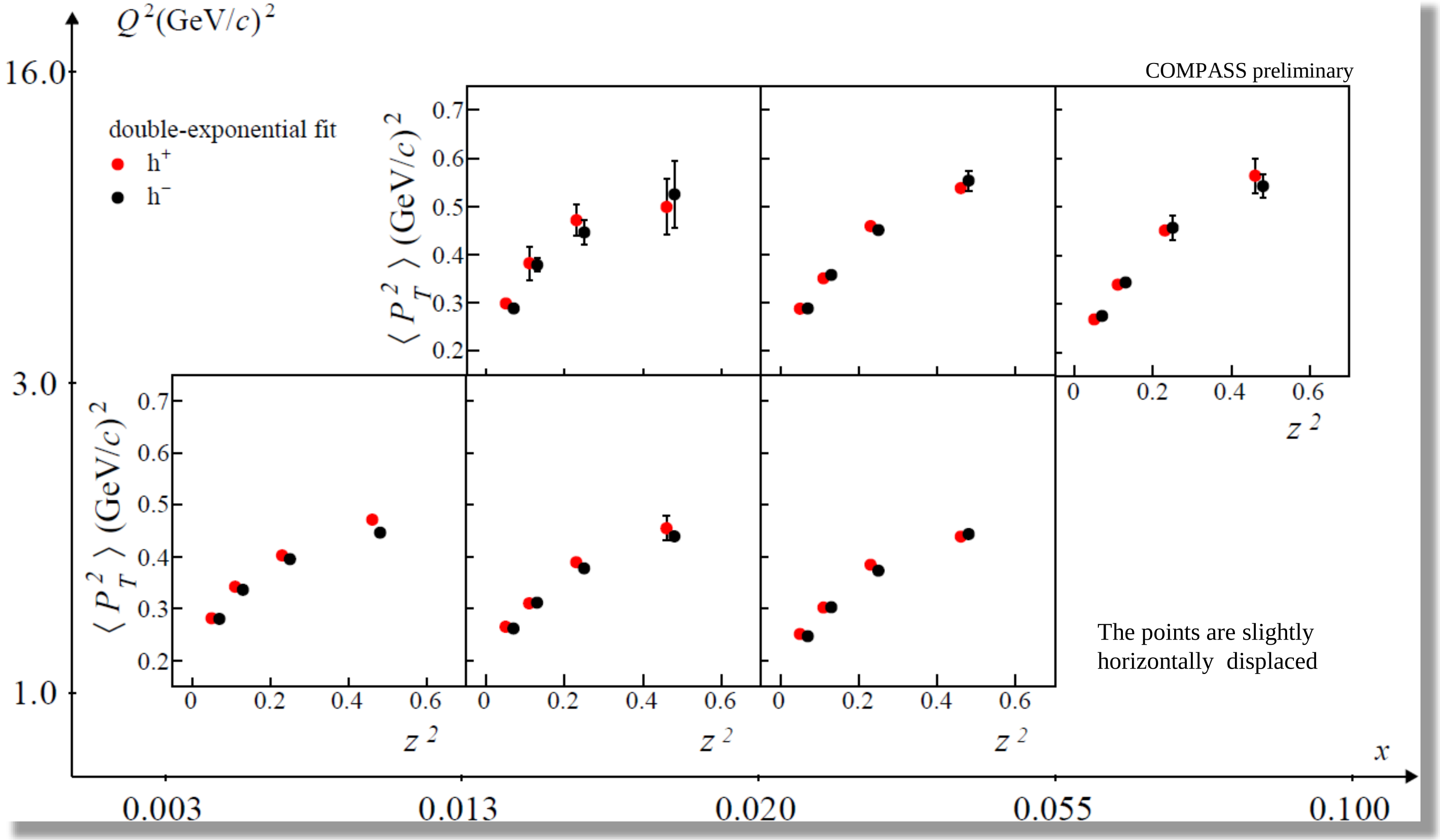

Fit of the P_T^2 - distributions

Leading Order expectation: $\langle P_T^2 \rangle = z^2 \langle k_T^2 \rangle + \langle p_\perp^2 \rangle$
Deviation from linearity: already there with the deuteron multiplicities / distributions

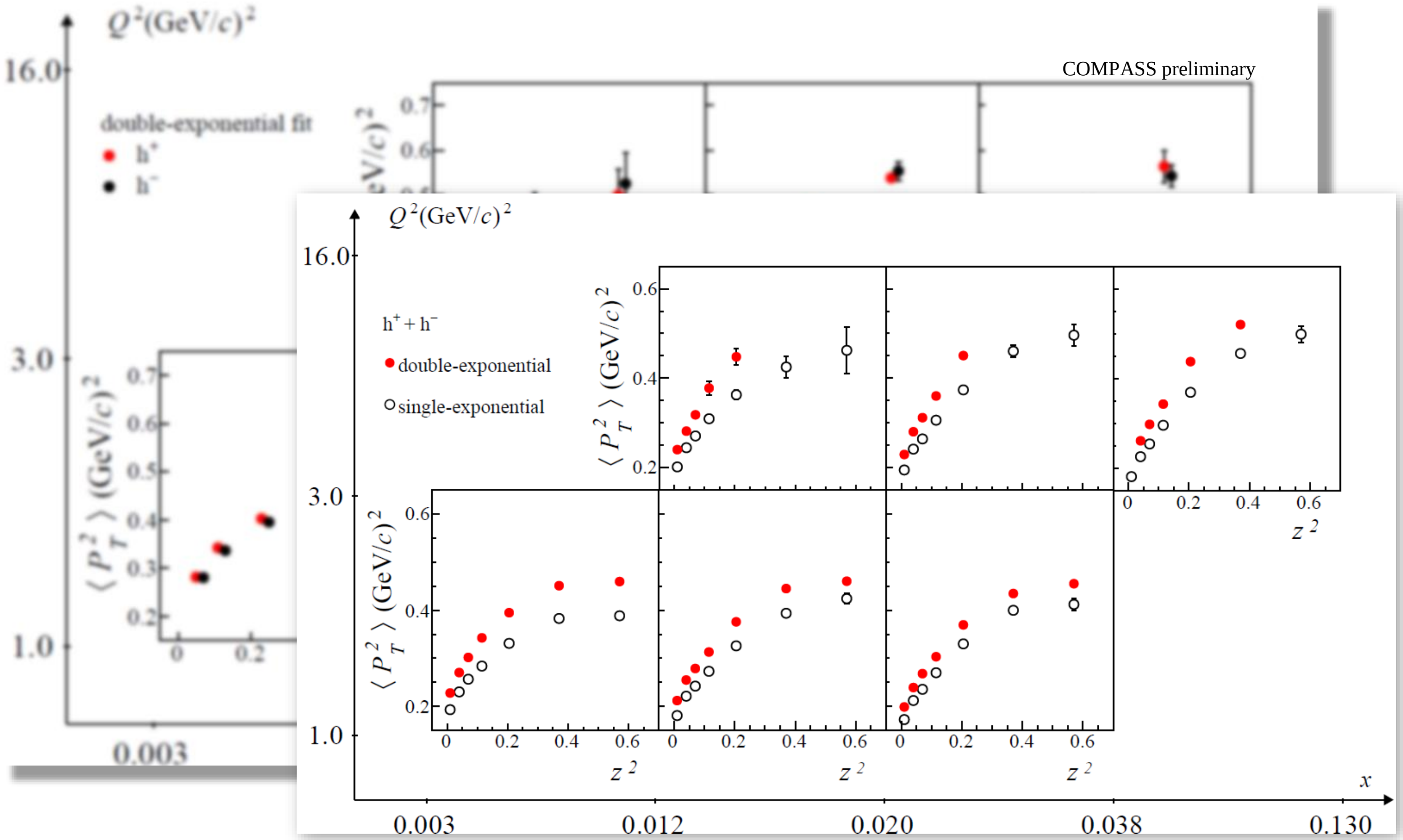

Kinematic dependences

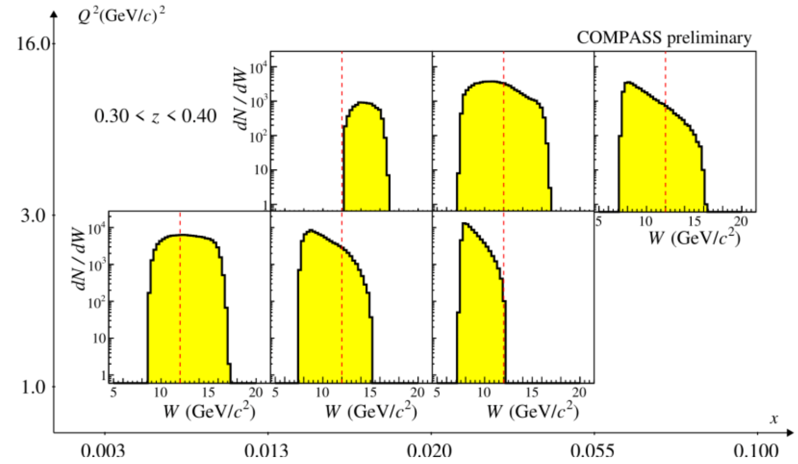

Investigation of kinematic dependences on Q^2, W

- *Distributions in 2 W bins + ratio high-over-low Q^2 + ratio high-over-low W*
- *Distributions in 4 Q^2 bins*
- *…*

Interesting observation: increase of $\langle P_T^2 \rangle$ with W

Phase-space effect

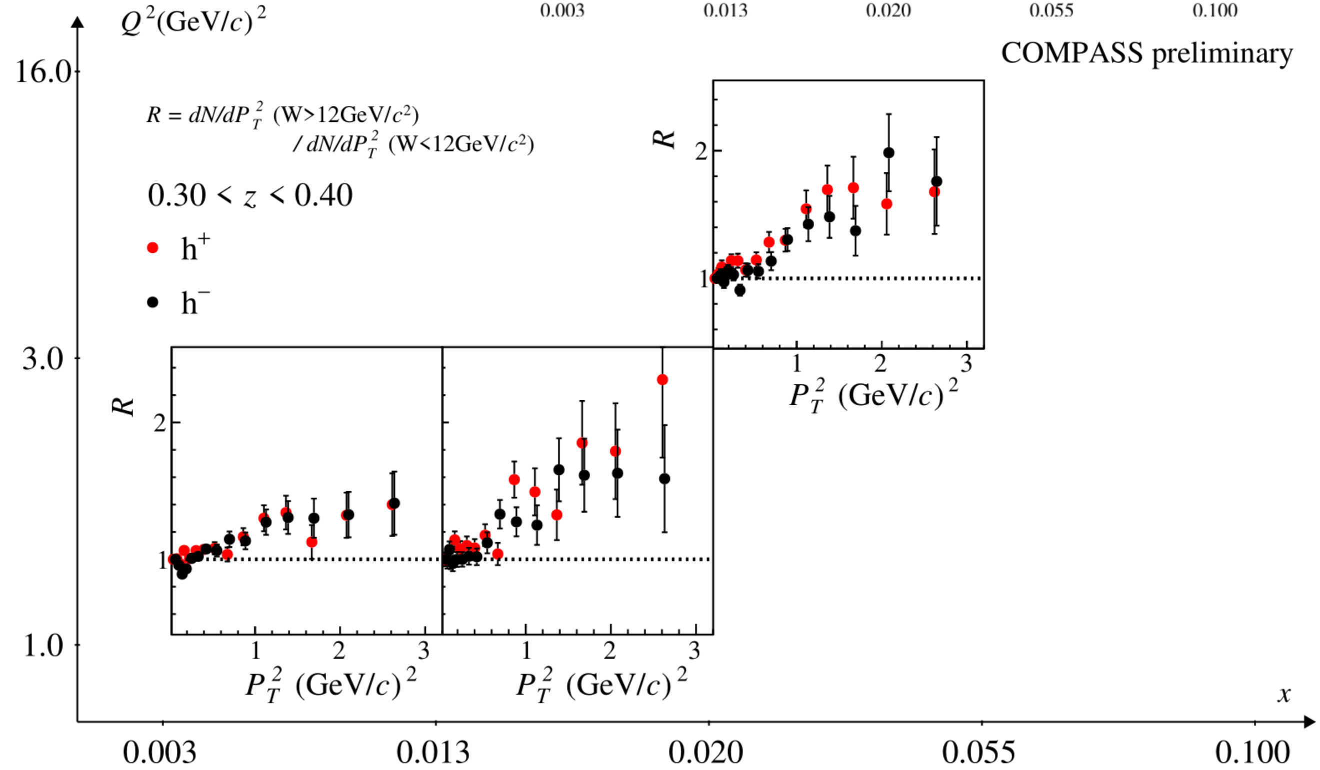

Azimuthal asymmetries – 1D

Azimuthal asymmetries: defined as the following ratios

$$A_{UU}^{\cos\phi_h} = \frac{F_{UU}^{\cos\phi_h}}{F_{UU,T}} \qquad A_{UU}^{\cos 2\phi_h} = \frac{F_{UU}^{\cos 2\phi_h}}{F_{UU,T}} \qquad A_{LU}^{\sin\phi_h} = \frac{F_{LU}^{\sin\phi_h}}{F_{UU,T}}$$

Steps in the measurement:

1. Exclusive hadrons:
   - the visible component is *discarded*
   - the non-visible component is *subtracted* using the HEPGEN Monte Carlo
2. Acceptance correction
3. Fit of the **amplitude of the modulation in the azimuthal angle** of the hadrons
   - as a function of x, z or P_T (1D)
   - with a simultaneous binning (3D)

- **Strong kinematic dependences**
- **Interesting differences** between positive and negative hadrons, as observed in previous measurements by COMPASS on deuteron and by HERMES

COMPASS preliminary

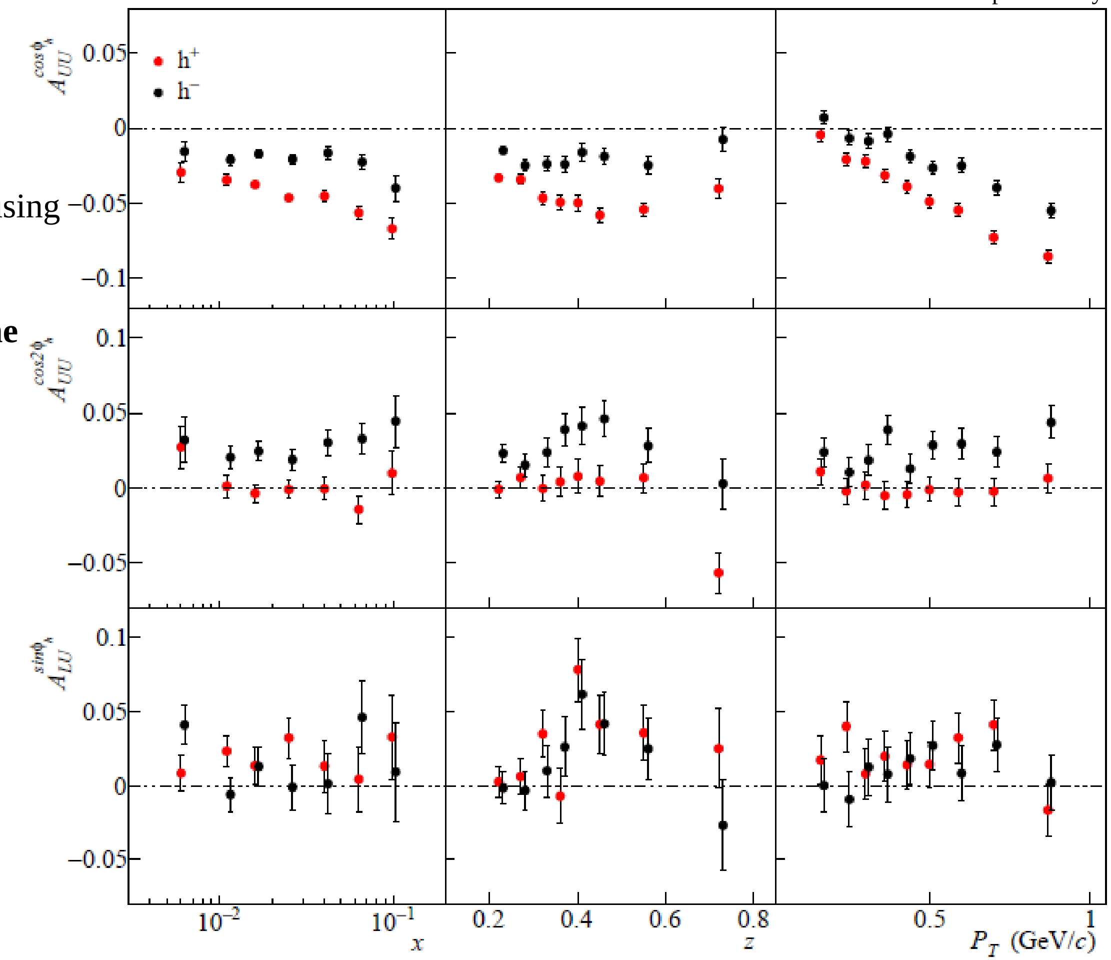

The error bars correspond to the statistical uncertainty only. $\sigma_{syst} \sim \sigma_{stat}$ (1D)

Azimuthal asymmetries – 3D – $A_{UU}^{cos\phi_h}$

The error bars correspond to the statistical uncertainty only. $\sigma_{syst} \sim 0.5\, \sigma_{stat}$ (3D)

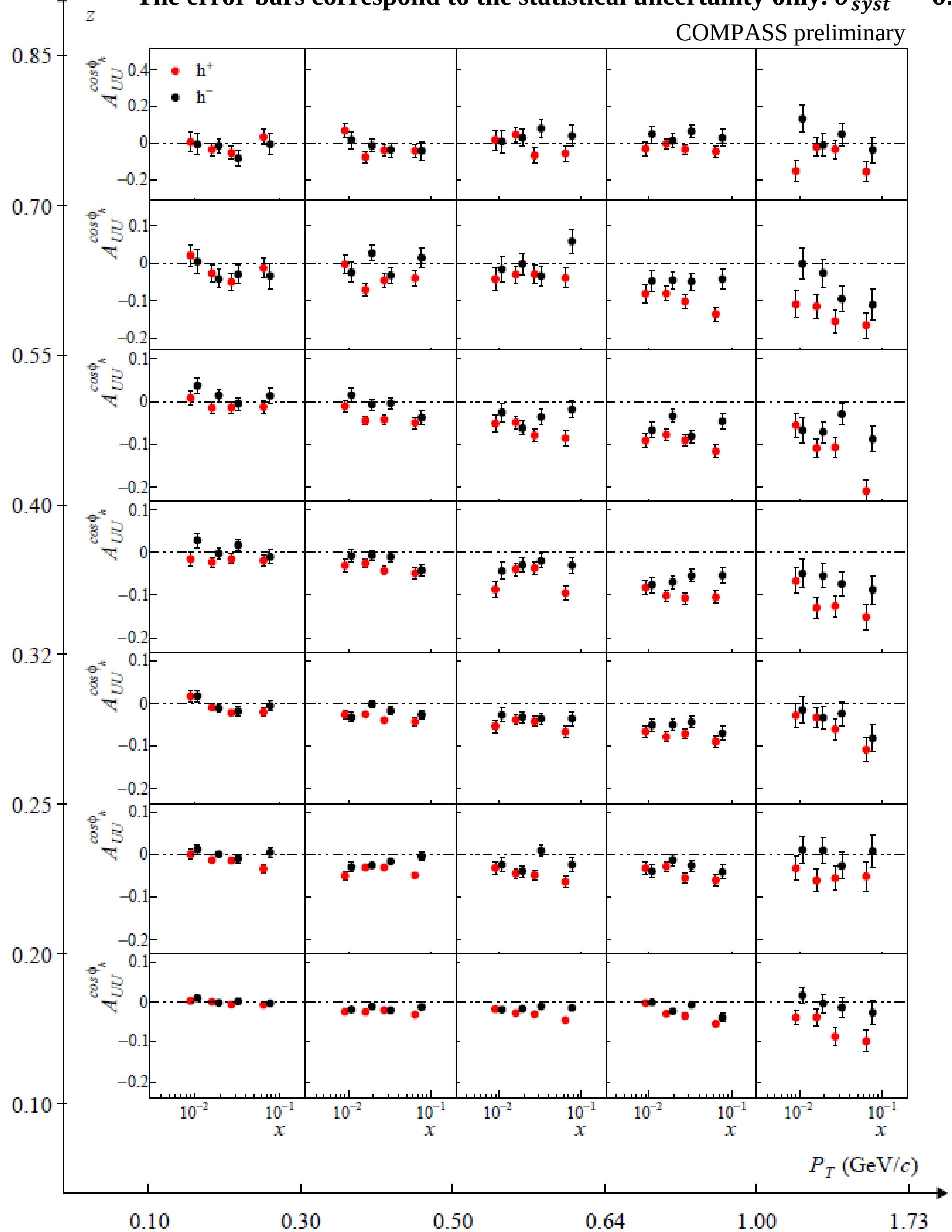

3D azimuthal asymmetries for positive and negative hadrons

Clear signal, strong dependence on P_T;
compatible with zero at high z.
In agreement with COMPASS deuteron results.

Expectation from Cahn effect:

$$A_{UU|Cahn}^{\cos\phi_h} = -\frac{2zP_T\langle k_T^2\rangle}{Q\,\langle P_T^2\rangle}$$

Comparison with the 1D case:
lowest z and highest P_T bin not included in the average

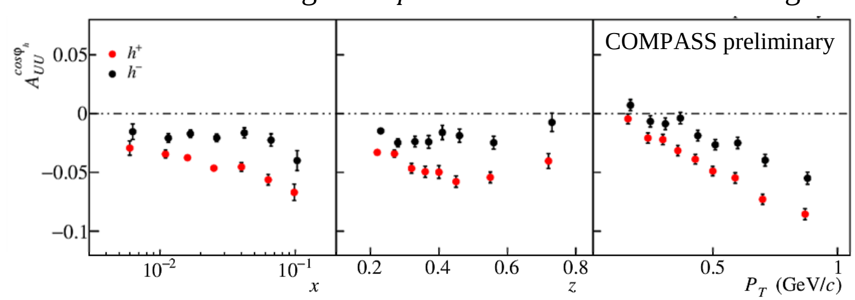

Extraction of $\langle k_T^2 \rangle$ from $A_{UU}^{\cos\phi_h}$

Extraction of $\langle k_T^2 \rangle$
from the 1D – asymmetry
assuming only Cahn effect
at work

$$\langle k_T^2 \rangle_{eff} = -\frac{Q\langle P_T^2 \rangle A_{UU}^{\cos\phi_h}}{2zP_T}$$

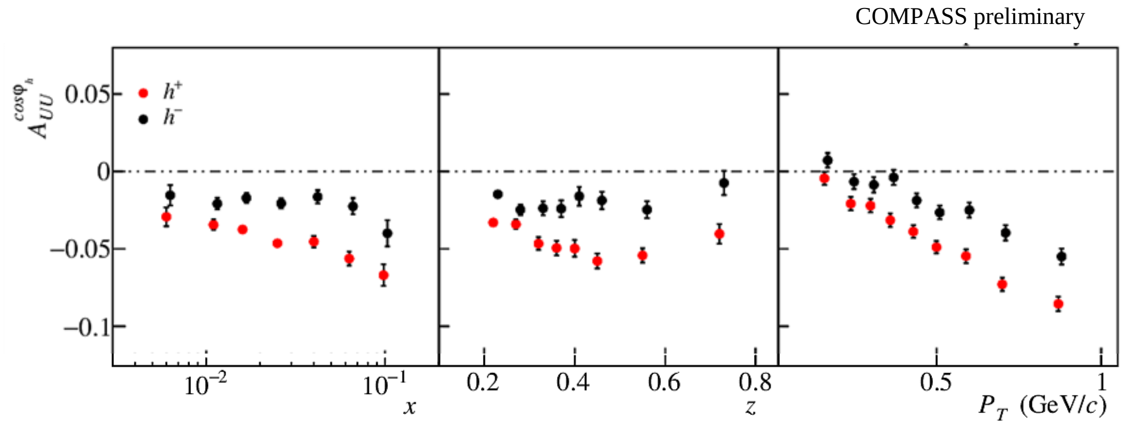

Power-law fit of $\langle k_T^2 \rangle(x)$

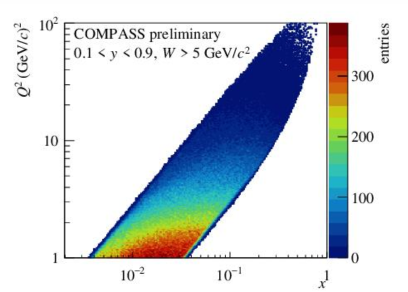

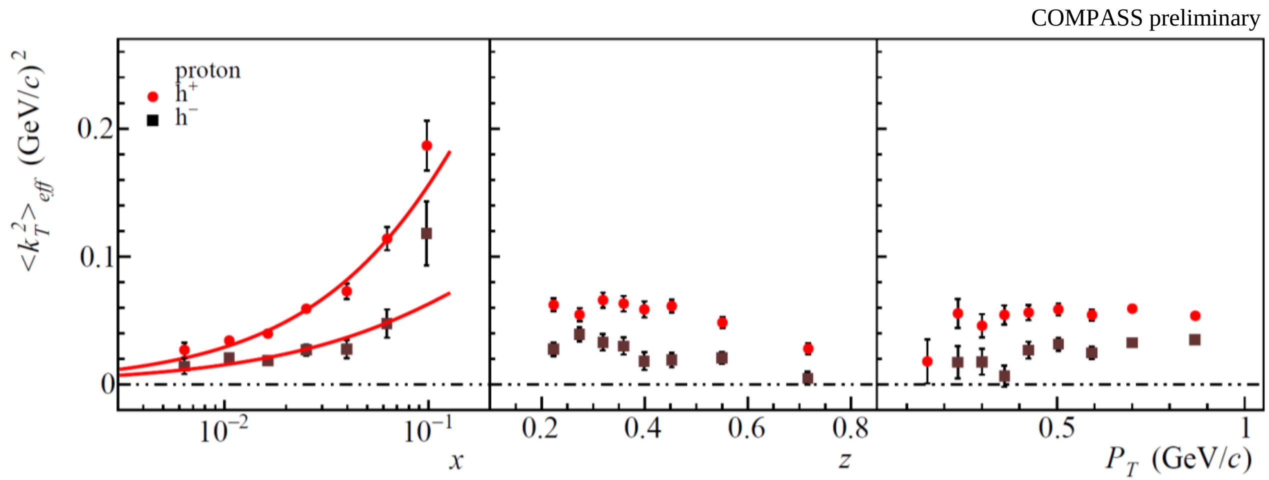

Is it an x – or Q^2 – dependence (or both)?

Azimuthal asymmetries – 1D – Q^2 dependence

Binning in Q^2

- Flavor-independent expectation from the Cahn effect:

$$A_{UU|Cahn}^{\cos\phi_h} = -\frac{2zP_T\langle k_T^2\rangle}{Q\,\langle P_T^2\rangle}$$

- The $A_{UU}^{cos\phi_h}$ asymmetry is observed to increase with Q^2 ***unexpected!***
- The difference between positive and negative hadrons decreases with Q^2.
- **Almost no Q^2 dependence for $A_{UU}^{cos2\phi_h}$**

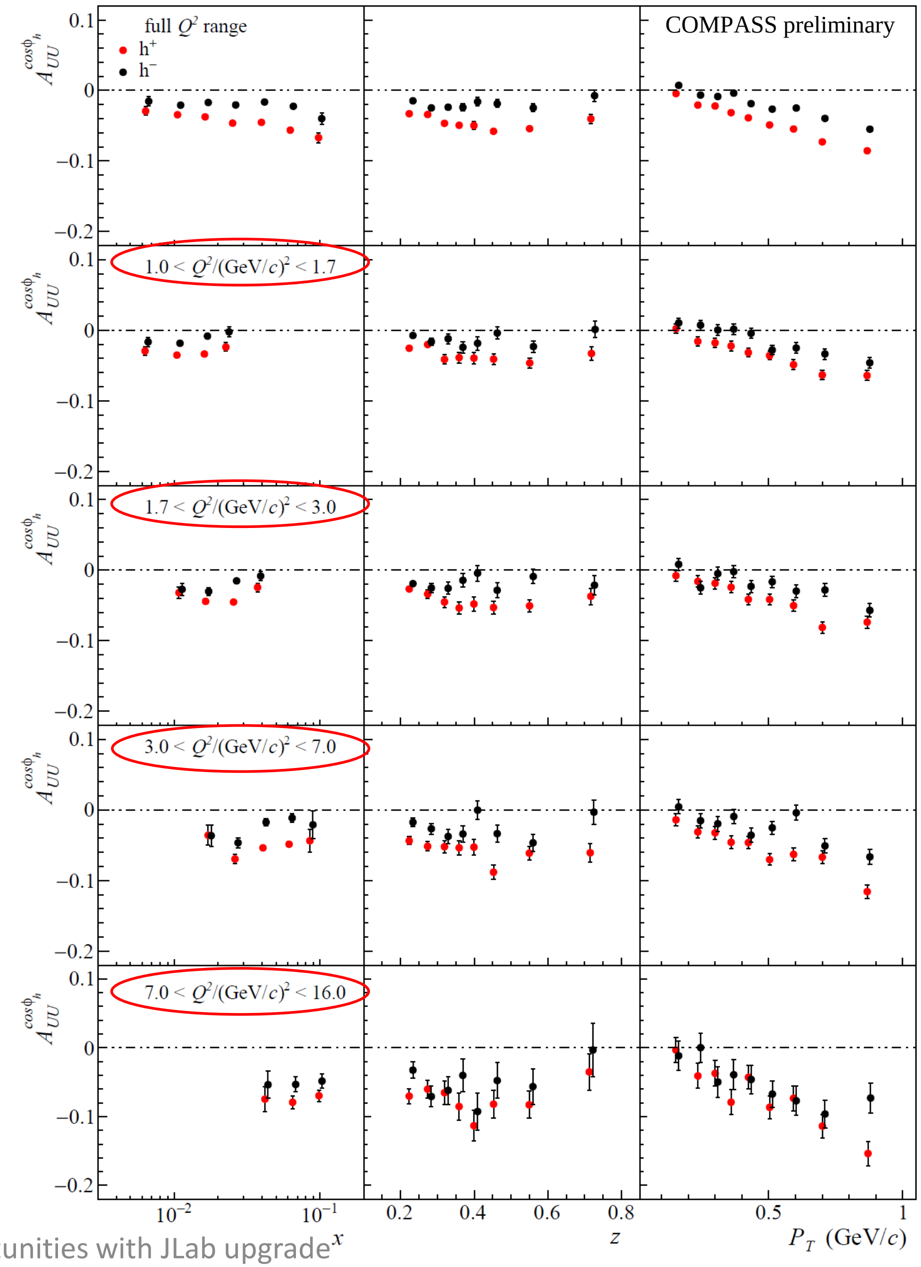

Extraction of $\langle k_T^2 \rangle$ from $A_{UU}^{\cos\phi_h}$

Extraction of $\langle k_T^2 \rangle$ *assuming only Cahn effect at work*

$$\langle k_T^2 \rangle_{eff} = -\frac{Q \langle P_T^2 \rangle A_{UU}^{\cos\phi_h}}{2 z P_T}$$

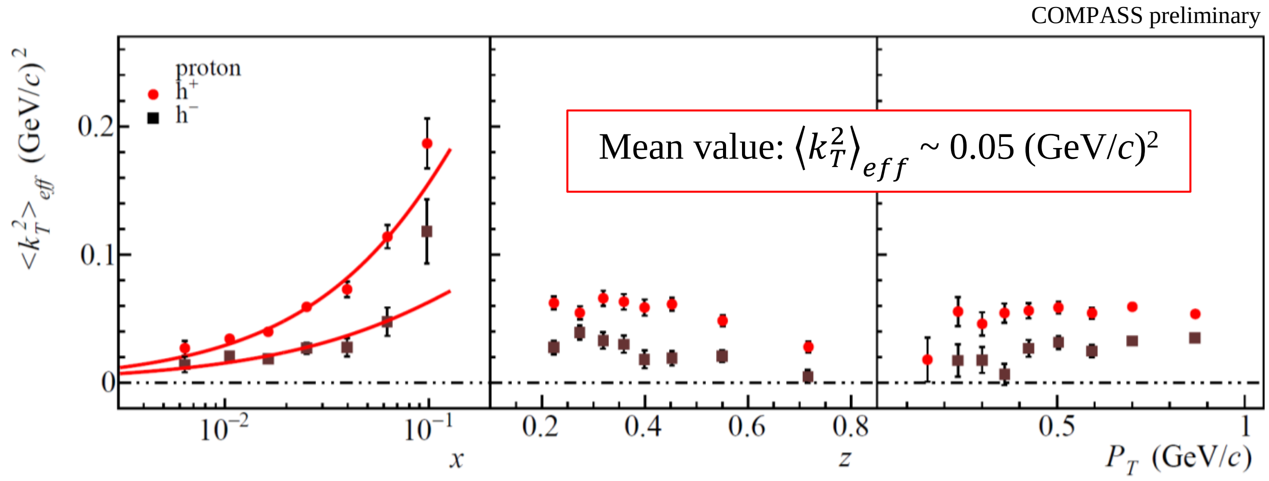

$\langle k_T^2 \rangle$ almost constant in x, strong Q^2 dependence

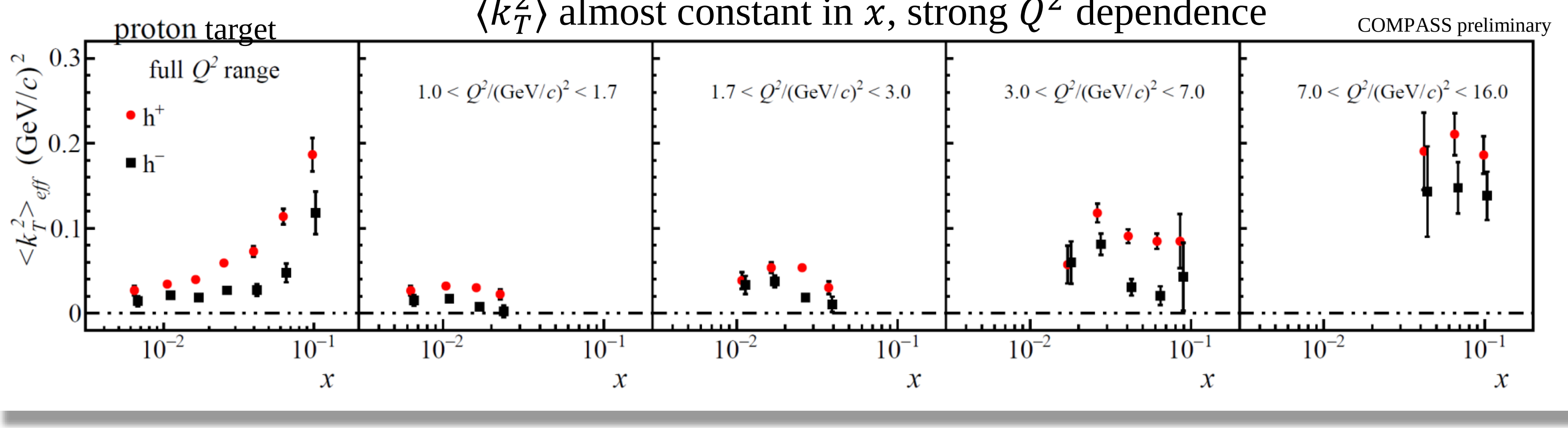

Azimuthal asymmetries – 3D – $A_{UU}^{cos2\phi_h}$

The error bars correspond to the statistical uncertainty only. $\sigma_{syst} \sim 0.5\,\sigma_{stat}$ (3D)

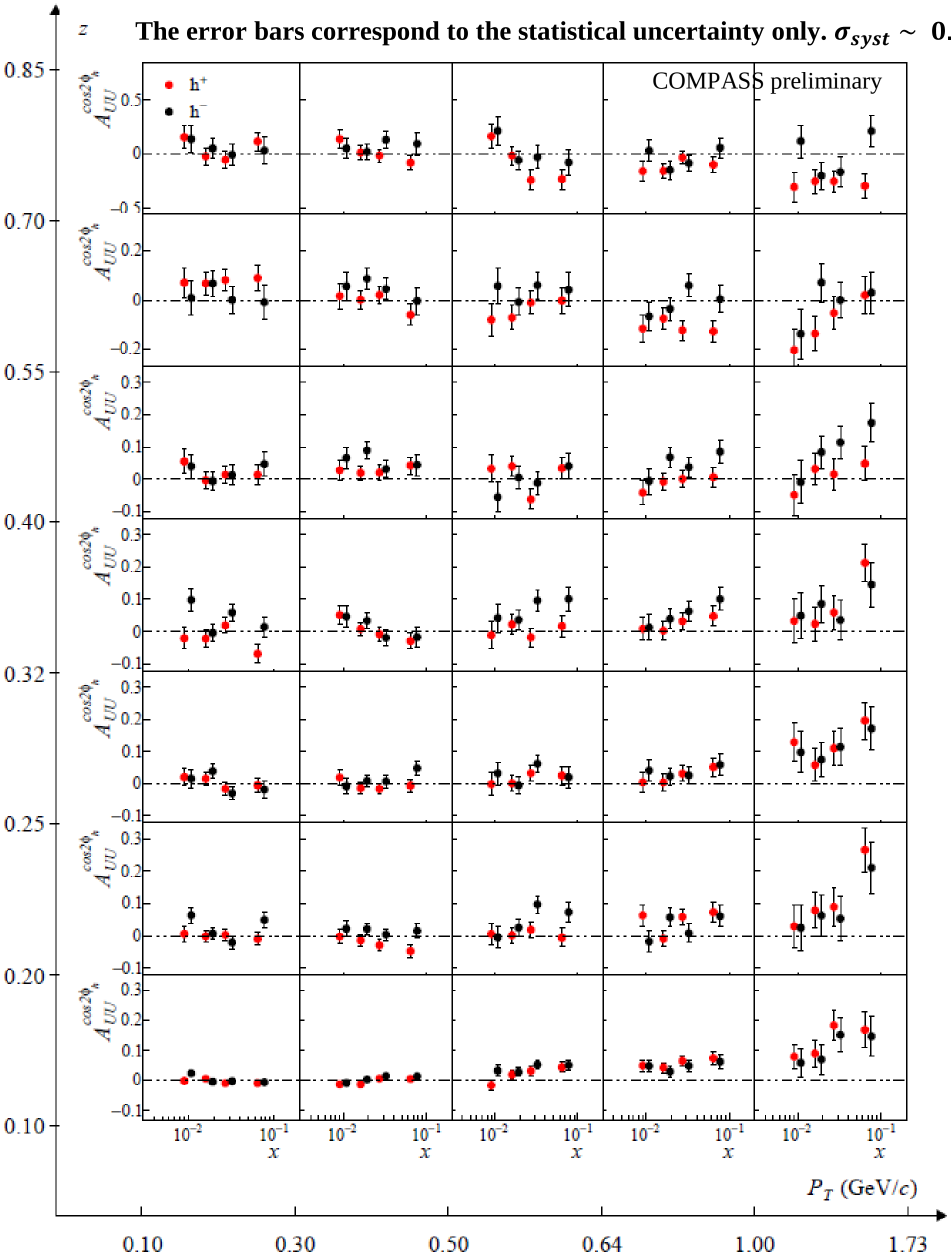

3D azimuthal asymmetries for positive and negative hadrons

Clear signal, strong dependence on x and P_T; interesting change of sign along z at high P_T.

The larger contribution from the $h_1^\perp H_1^\perp$ convolution → direct information on $h_1^\perp$ may be extracted

Comparison with the 1D case:
lowest z and highest P_T bin not included in the average

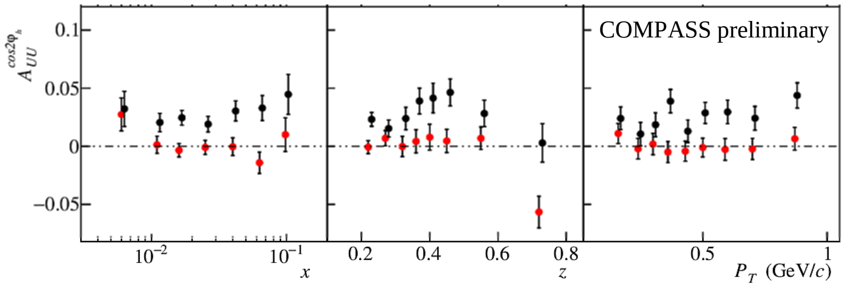

A rich program

P_T^2-distributions

- *For positive and negative hadrons in bins of x, Q^2 and z (4,2,4)*
- *Fits with single exponential, double exponential and Tsallis*
- *$\langle P_T^2 \rangle$ vs. z^2 as from the double exponential fit*
- *Fit of $\langle P_T^2 \rangle$ vs. z^2 in bins of x, Q^2 and z*
- *Distributions in q_T and q_T^2*
- *Distributions in 2 W bins + ratio high-over-low Q^2 + ratio high-over-low W*
- *Distributions in 4 Q^2 bins*

Azimuthal asymmetries $A_{UU}^{\cos\phi_h}, A_{UU}^{\cos 2\phi_h}$ and $A_{LU}^{\sin\phi_h}$

- *1D: standard binning in x, z or P_T*
- *Also: low-z and high-P_T -- for completeness*
- *1D standard + 4 bins in Q^2: interesting evolution of $A_{UU}^{\cos\phi_h}$*
- *1D standard + 2 bins in Q^2 and 2 bins in W*
- *3D: standard binning (simultaneous in x, z and P_T)*
- *In addition to deuteron analysis: low-z bin*

New: Dihadron azimuthal asymmetries $A_{UU}^{\cos 2\phi_{hh}}, A_{UU}^{\cos(\phi_{hn}-\phi_R)}, A_{UU}^{\cos\phi_R}$ and $A_{UU}^{\cos\phi_{hh}}$

- *1D: standard binning in x, z or P_T*
- *Focus on Boer-Mulders related asymmetries*
- *Shown at Transversity 2022 and IWHSS 2022*

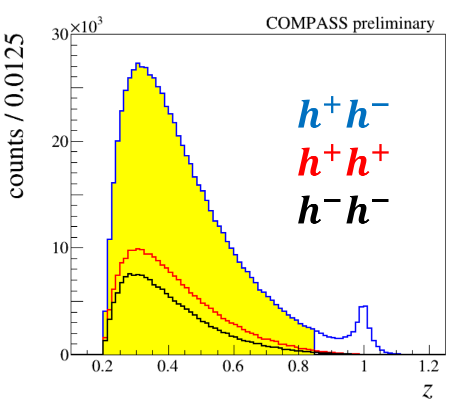

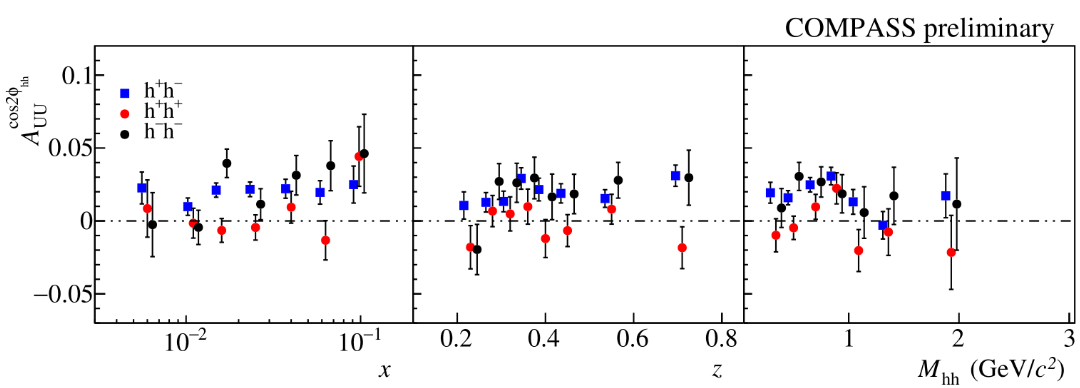

Conclusions and Perspectives

- **Transverse momentum distributions** and **azimuthal asymmetries:**
  "fundamental" observables to access the nucleon structure in unpolarized SIDIS

- **COMPASS** has produced new results for both of them, using a **proton** target
  Here a selection of the main results and a "flash" of new 2h results

- Intriguing investigations of their properties:
  rich kinematic dependences, h^+h^- differences, …

Still a lot to be understood and/or addressed

- Difference between positive and negative hadrons in azimuthal asymmetries
  – but same P_T^2-slopes
- Kinematic dependences (sometimes *counterintuitive* for azimuthal asymmetries)
- Impact of phase-space limitations in the production of hadrons (for the P_T-distributions)
- Role of twist-3 contributions
- Impact of radiative corrections
  may be relevant e.g. for the Q^2 dependence of the azimuthal asymmetries
- Role of vector mesons inclusively produced in SIDIS
  particularly for their contribution to the P_T^2 - distributions at low P_T

backup

Comparison with Pavia fit (PV-17)

Comparison with the predictions of the P_T-dependent SIDIS cross section as from PV-17 [A. Bacchetta et al., JHEP 06 (2017) 081]

PV-17:
- SIDIS $ep(D) \rightarrow e\pi^{\pm}(K^{\pm})X$ (HERMES)
- SIDIS $\mu D \rightarrow \mu h^{\pm} X$ (COMPASS)
- Drell-Yan (E228, E605)
- Z boson production (CDF, D0)

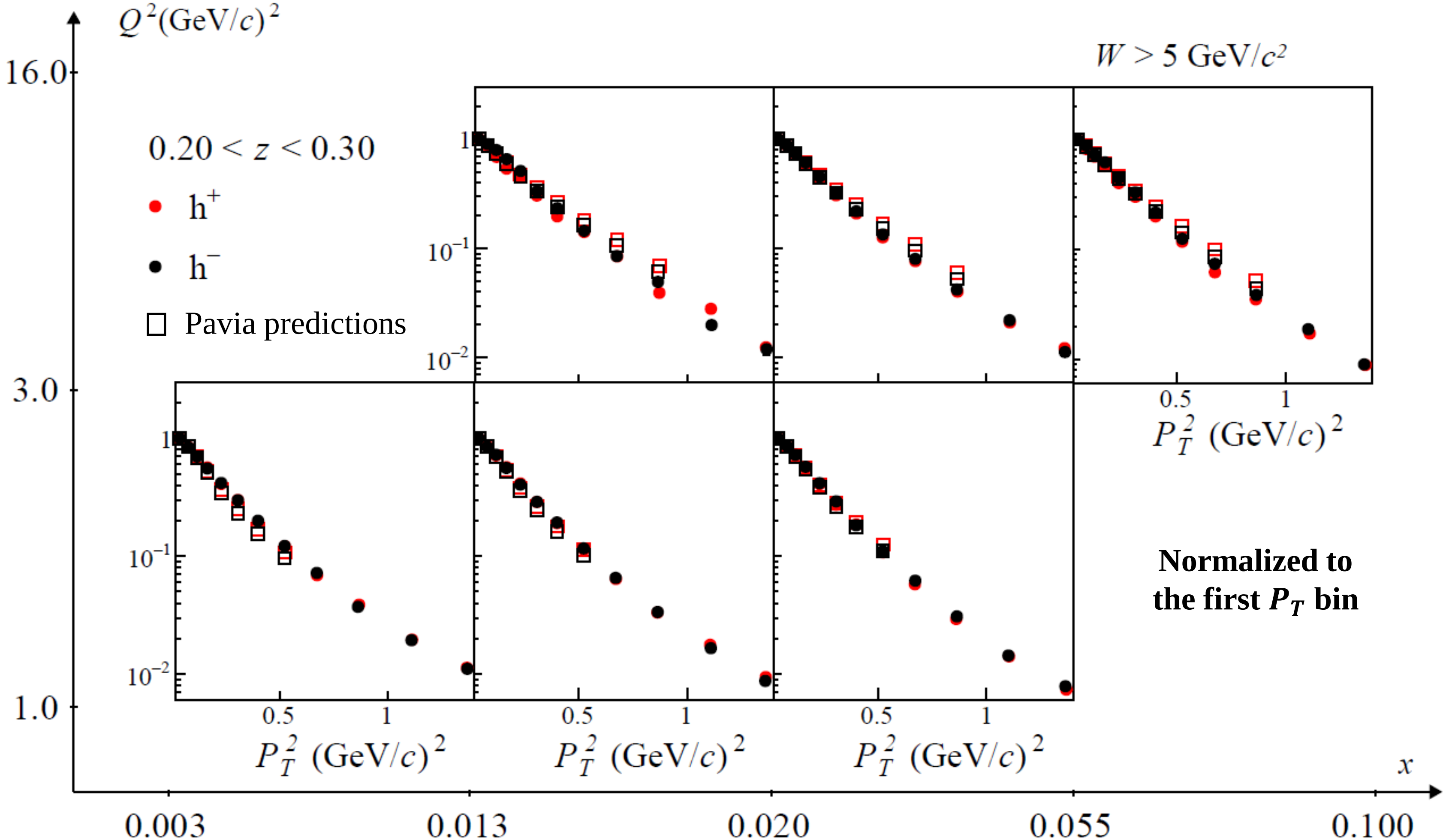

Comparison with Pavia fit (PV-17)

□ Pavia predictions

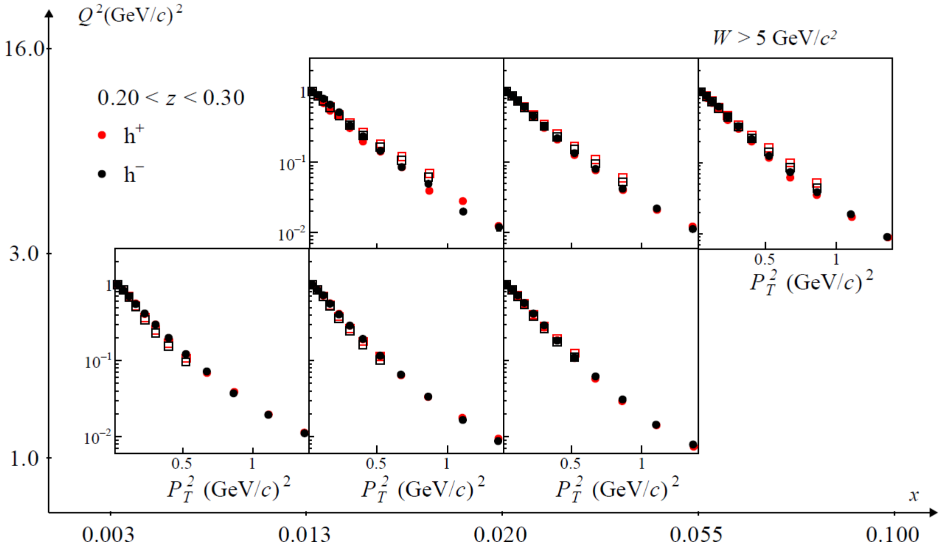

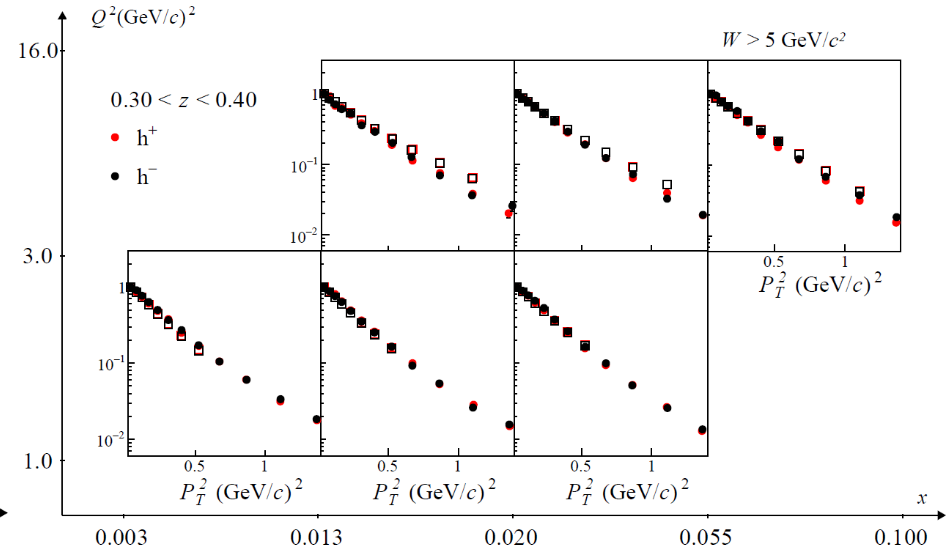

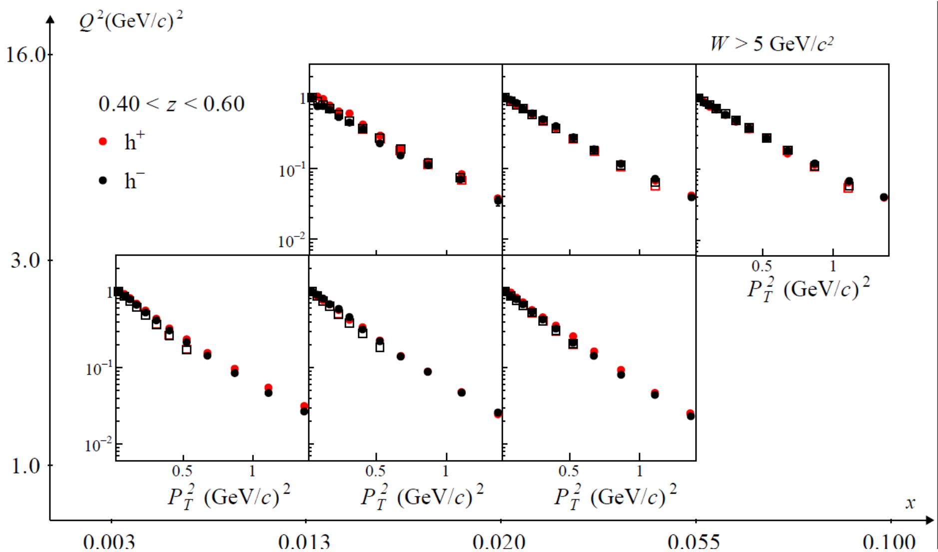

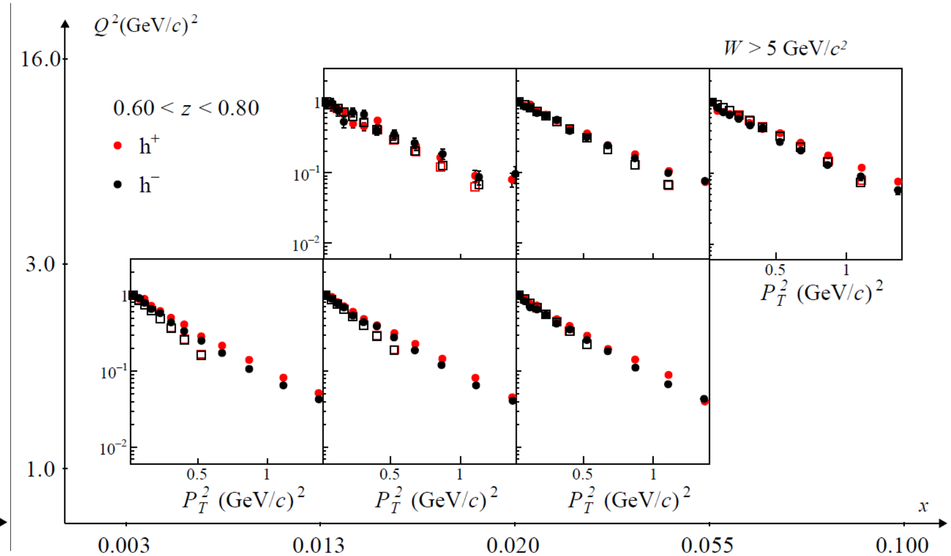

Comparison with Pavia fit (PV-17)

- Pavia predictions

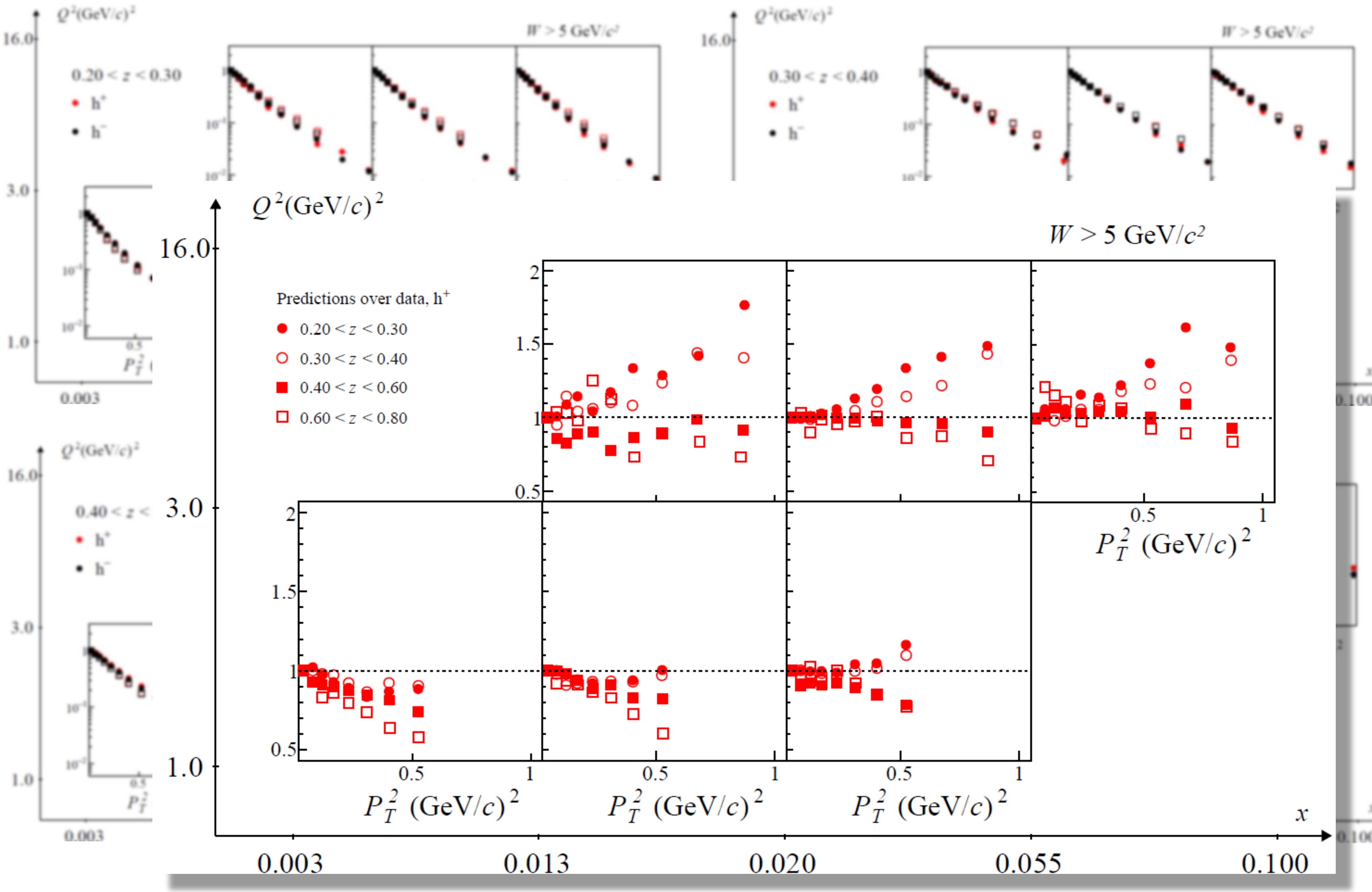

Comparison with Pavia fit (PV-17)

☐ Pavia predictions

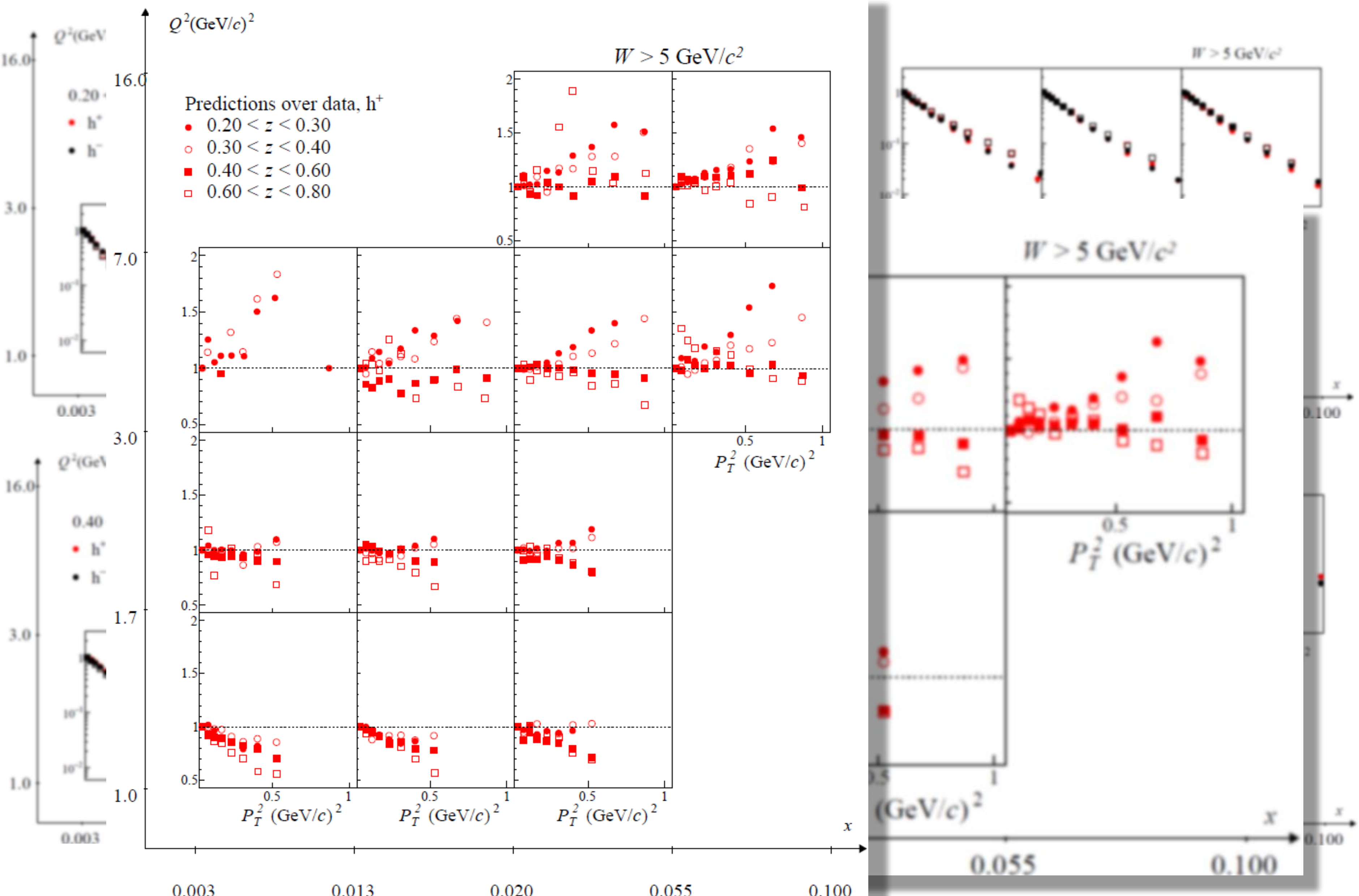

The 2016 COMPASS run

Events and hadron selection – standard

$Q^2 > 1\ (\mathrm{GeV}/c)^2$

$W > 5\ \mathrm{GeV}/c^2$

$0.003 < x < 0.130$

$0.2 < y < 0.9$

$\theta_\gamma < 60$ mrad

$z > 0.1$

$P_T > 0.1\ \mathrm{GeV}/c$

Size of the hadron sample: ~ 6.5 M hadrons

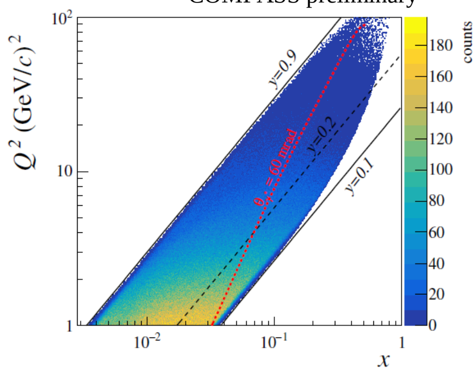

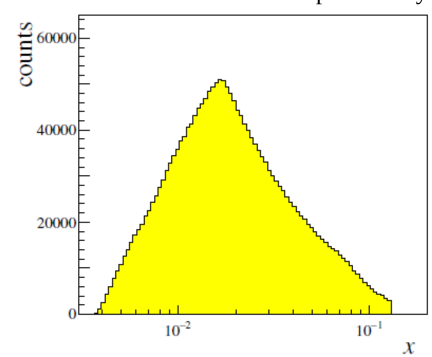

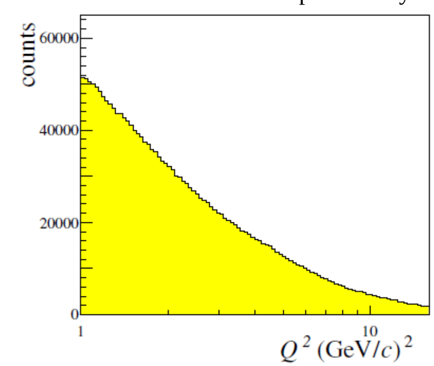

Comparison with the LEPTO Monte Carlo simulation.
Exclusive contribution at high *z* in the data

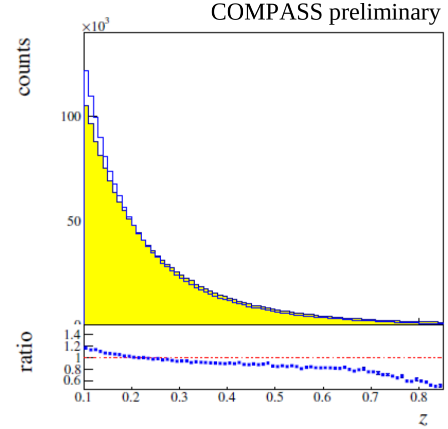

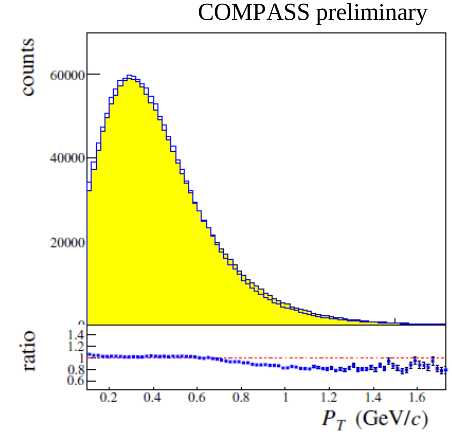

Contribution from exclusive hadrons

- The exclusive events fully reconstructed in the data are
  1) selected by cutting in missing energy E_{miss}
  2) used to normalized the HEPGEN Monte Carlo, needed to take into account the non-reconstructed part
  3) discarded
- The exclusive events non-fully reconstructed are subtracted using the normalized HEPGEN Monte Carlo
- This procedure does not require the knowledge of the absolute cross-section for the diffractive production, not well known (~ 30% relative uncertainty)

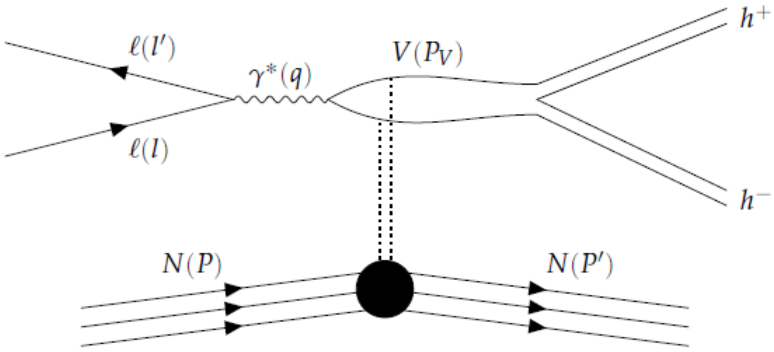

The diffractive production of a vector meson V and its decay into a hadron pair

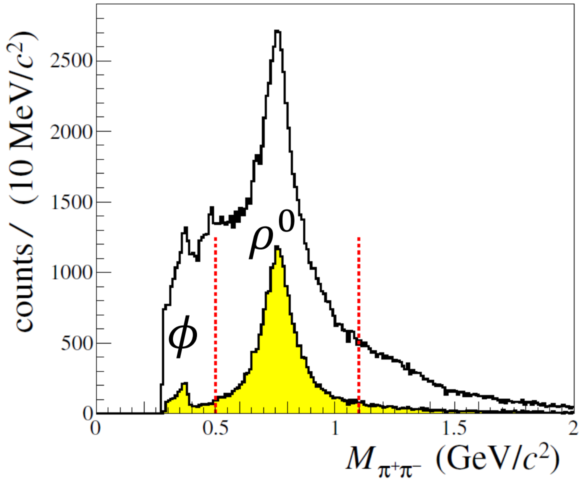

Invariant mass distribution in the data, before and after cutting in missing energy

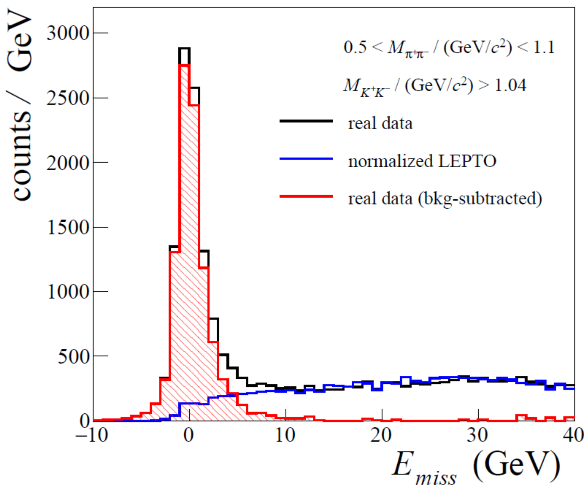

The exclusive peak as observed in the data

Contribution from exclusive hadrons

Estimated exclusive hadrons contaminations in the data:
~80% is fully reconstructed

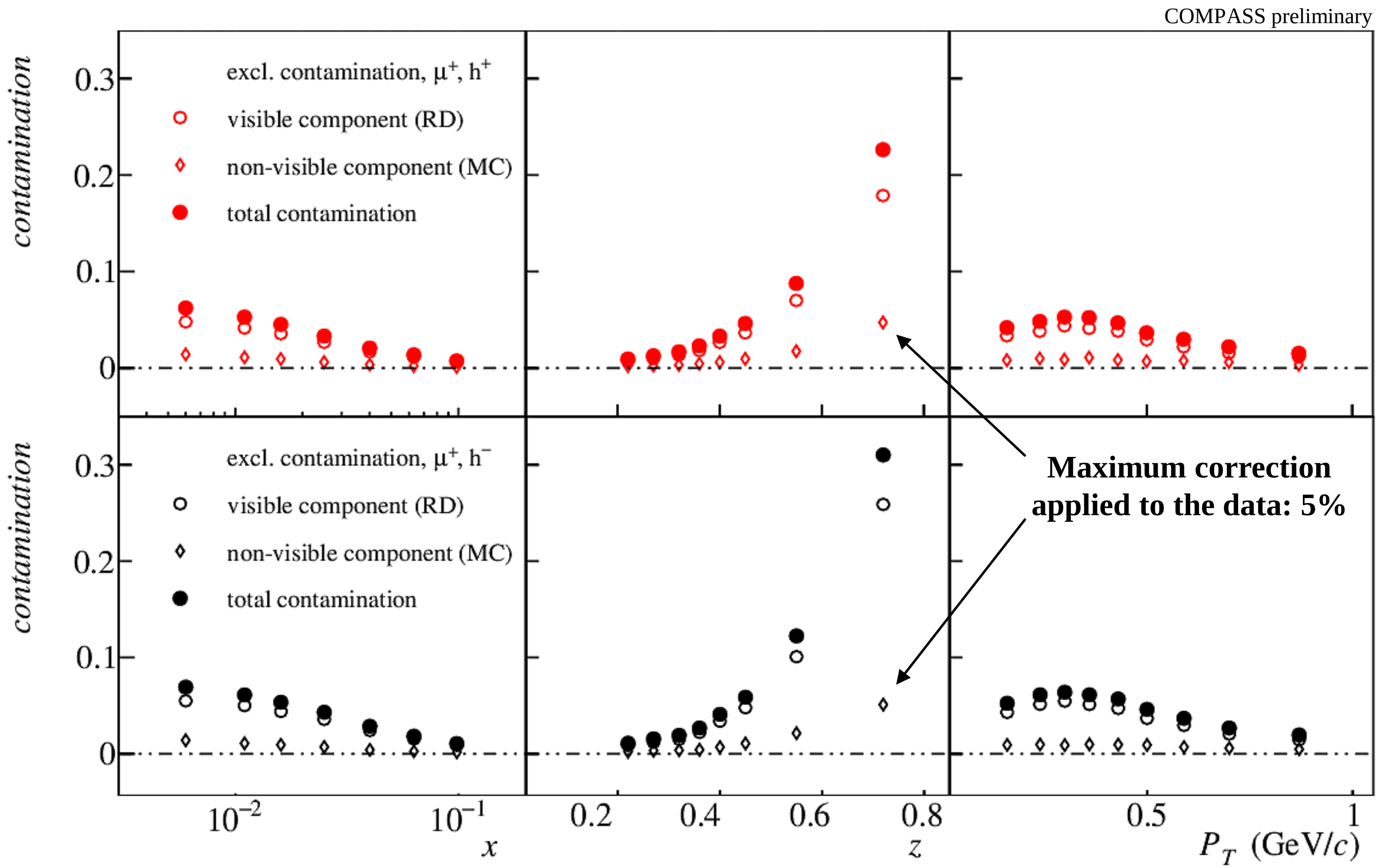

Extraction of $\langle k_T^2 \rangle$ from $A_{UU}^{\cos\phi_h}$

Extraction of $\langle k_T^2 \rangle$ *assuming only Cahn effect at work*

$$\langle k_T^2 \rangle_{eff} = -\frac{Q \langle P_T^2 \rangle A_{UU}^{\cos\phi_h}}{2zP_T}$$

Power-law fit of $\langle k_T^2 \rangle(x)$
Rather satisfactory description also vs z (below 0.5) and P_T

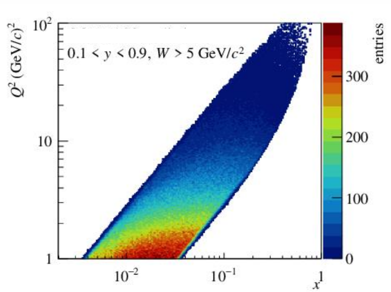

Is it an x − or Q^2 − dependence (or both)?

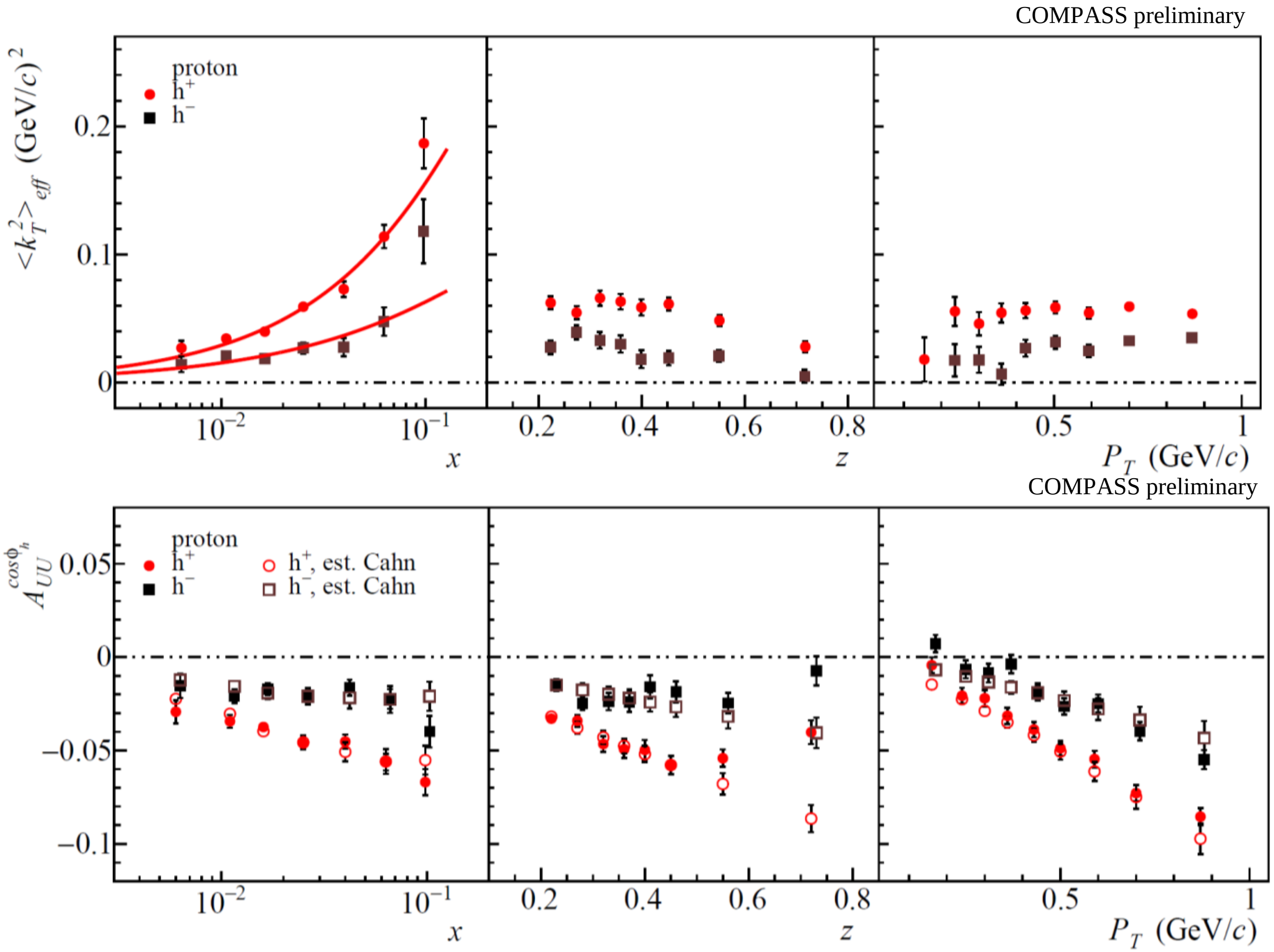

q_T distributions

- $q_T = P_T \,/\, z$, often indicated to set the limits of applicability of the TMD formalism
  (expected to hold at low q_T/Q)
- q_T distributions measured using the same hadron sample selected for the standard P_T^2 distributions
- Comparison with the approximated formula:

$$\frac{dN_h}{dz\, dP_T^2} = \frac{dN_h}{dz\, 2P_T dP_T} = \frac{dN_h}{dz\, dP_T\,/z} \frac{1}{2zP_T} \approx \frac{dN_h}{dz\, dq_T} \frac{1}{2zP_T}$$

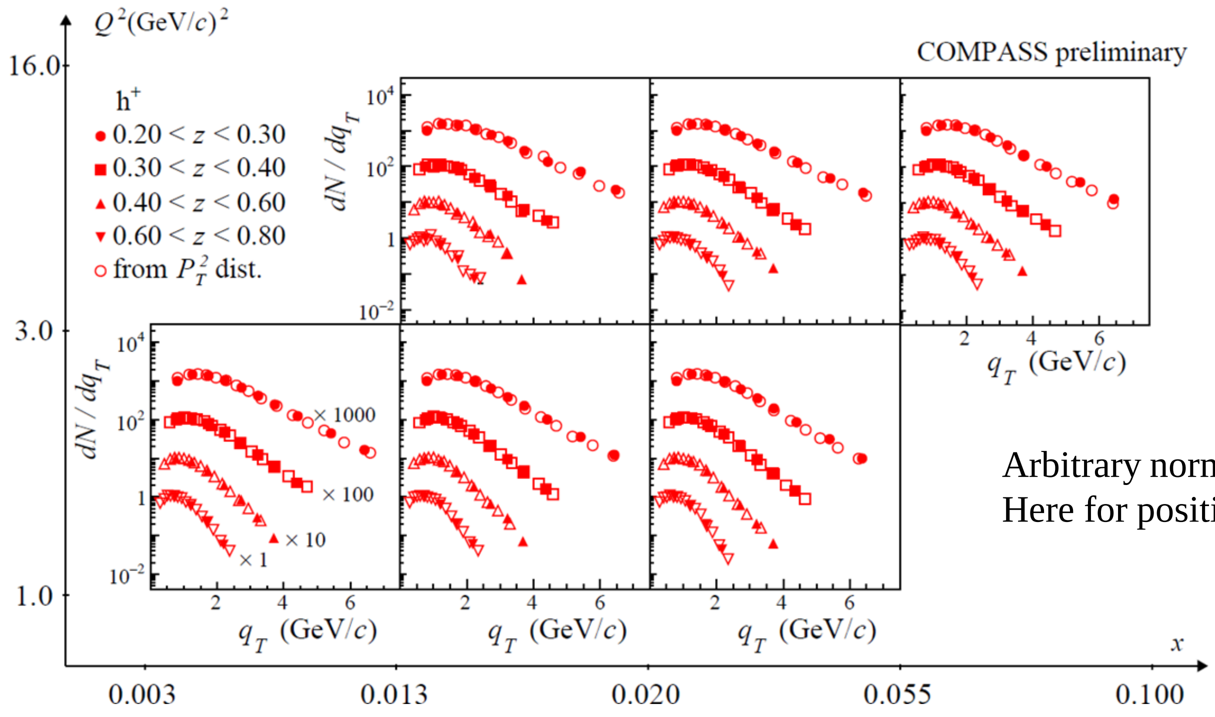

Arbitrary normalization and scaling
Here for positive hadrons, similar for negative

q_T^2 distributions

- $q_T = P_T / z$, often indicated to set the limits of applicability of the TMD formalism
  (expected to hold at low q_T/Q)
- q_T distributions measured using the same hadron sample selected for the standard P_T^2 distributions
- Comparison with the approximated formula:

$$\frac{dN_h}{dz\, dq_T^2} = \frac{dN_h}{dz\, 2q_T dq_T} = \frac{dN_h}{dz\, dq_T}\frac{1}{2q_T}$$

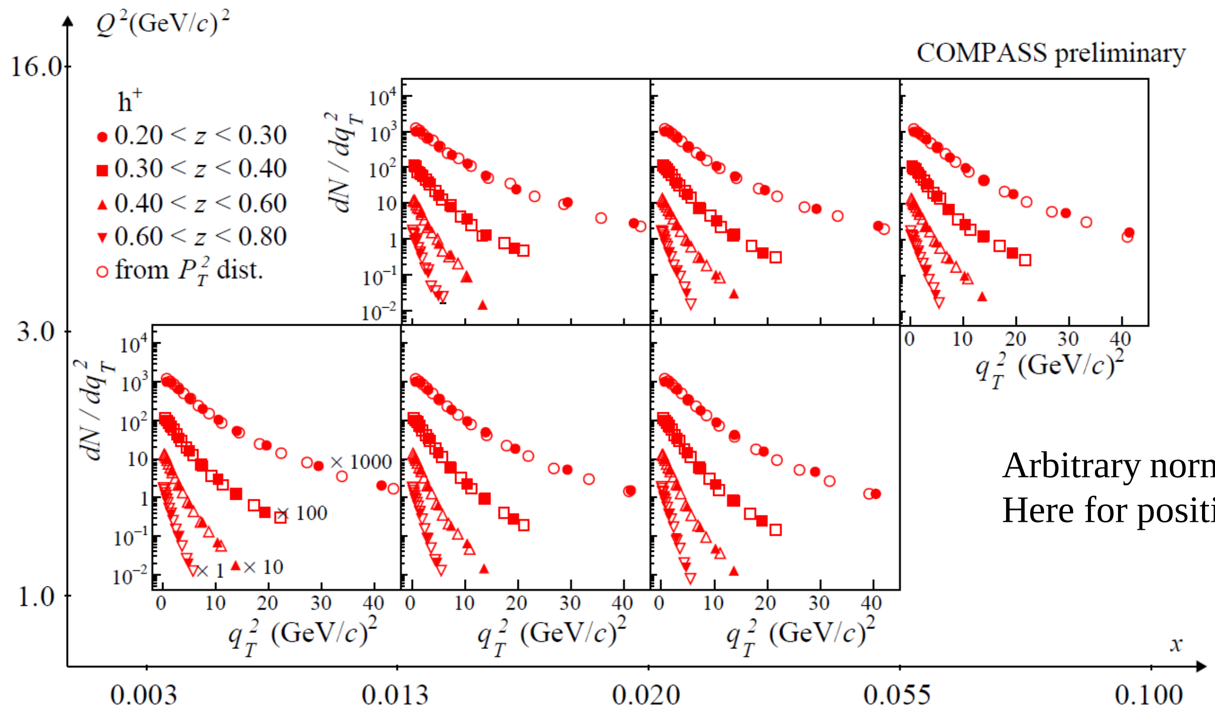

Arbitrary normalization and scaling
Here for positive hadrons, similar for negative

Acceptance modulations

Correction for acceptance applied to each ϕ bin, taken as the ratio of reconstructed and generated hadrons:

$$c_{acc}(\phi) = \frac{N_h^{rec}(\phi^{rec})}{N_h^{gen}(\phi^{gen})}$$

Azimuthal modulations of the acceptance in 1D binning, for μ^+ beam and positive (red) and negative hadrons (black).

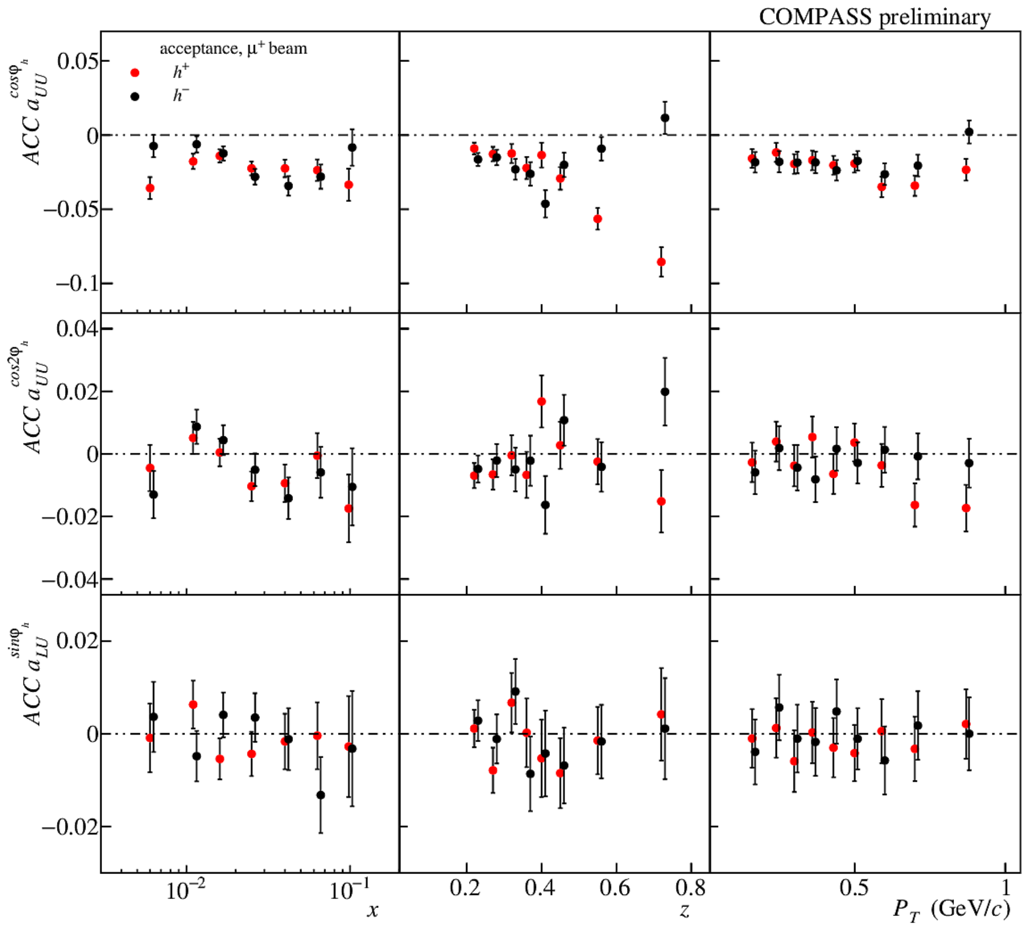

Acceptance modulations

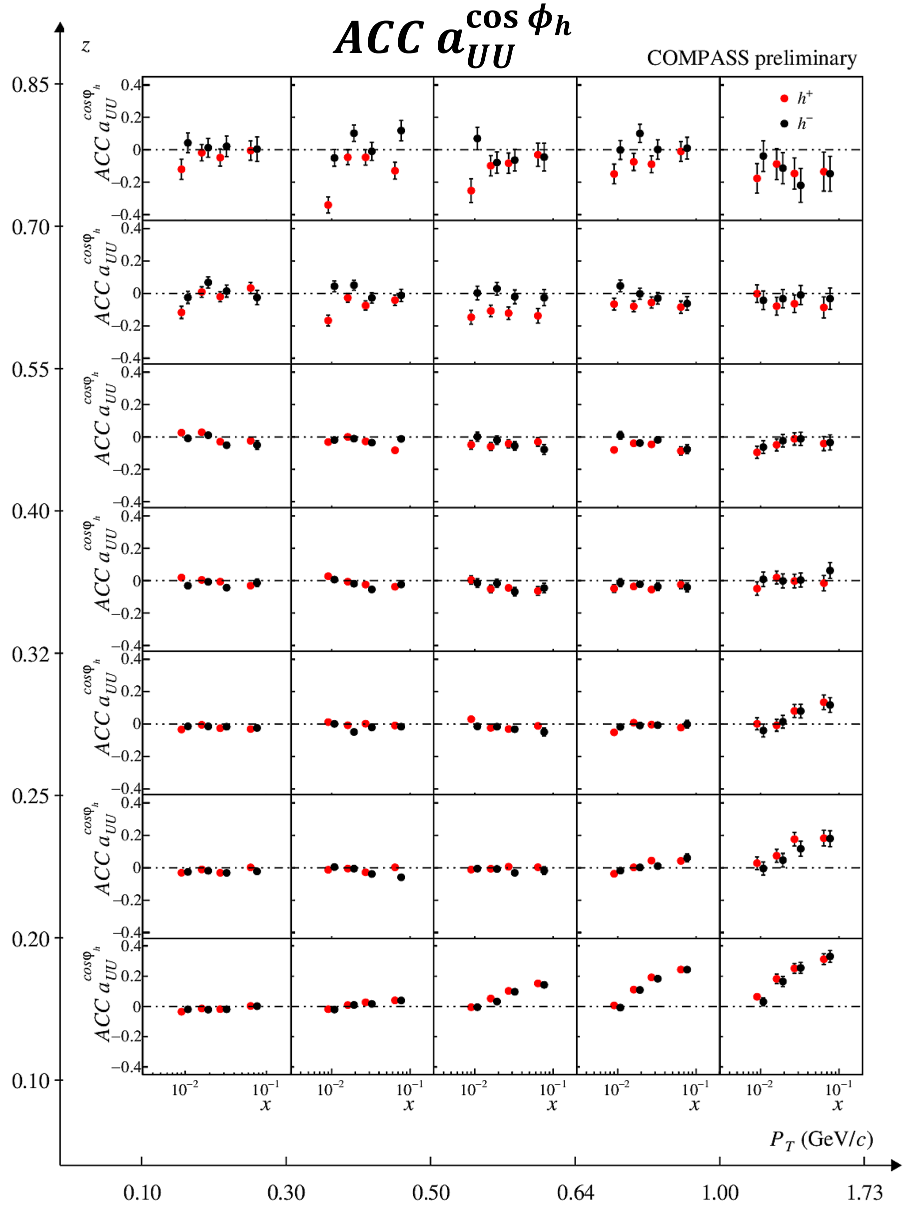

Azimuthal asymmetries – 3D

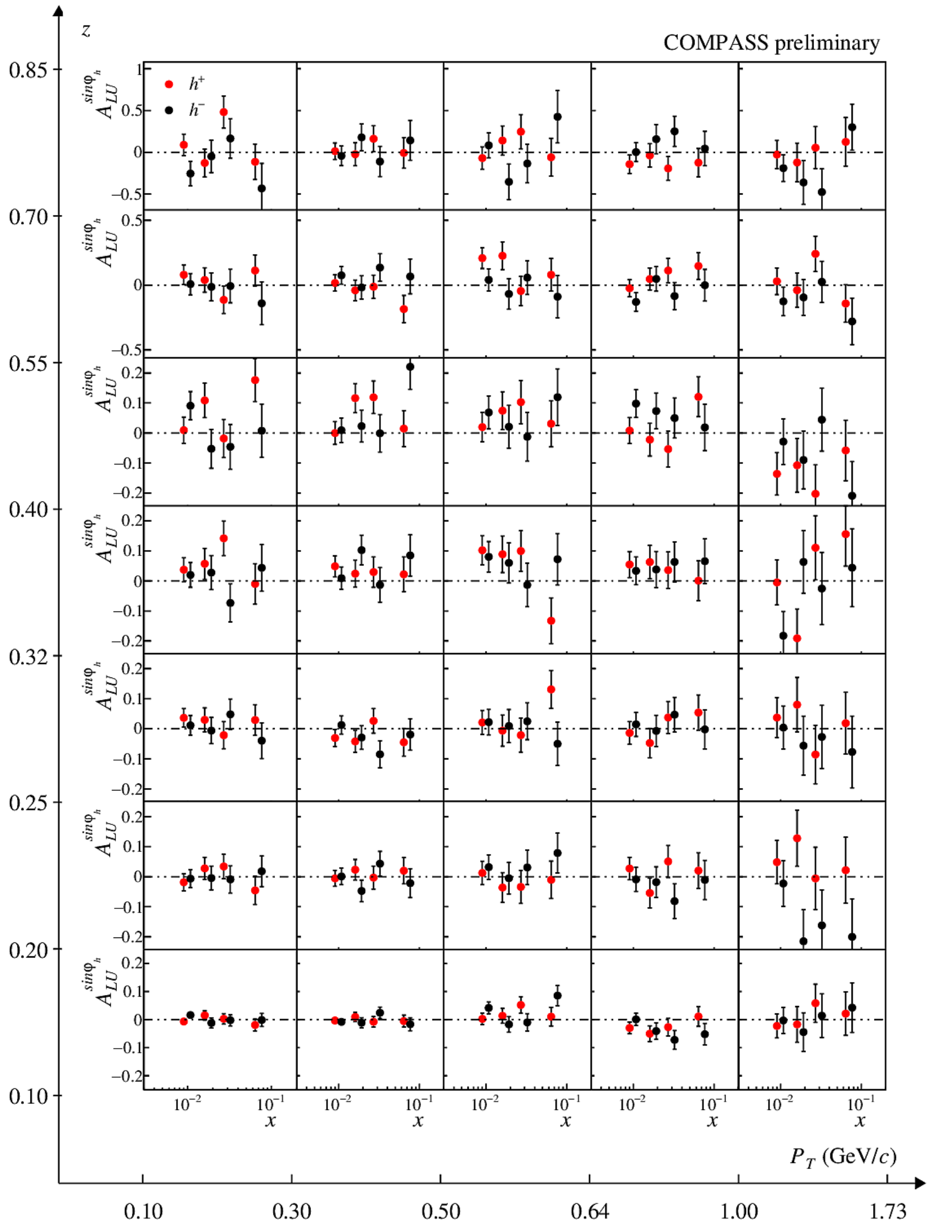

3D azimuthal asymmetries for positive and negative hadrons

$A_{LU}^{sin\phi_h}$ as a function of x,
in bins of z (rows) and P_T (columns).

Comparison with the 1D case:
lowest z and highest P_T bin not included in the average

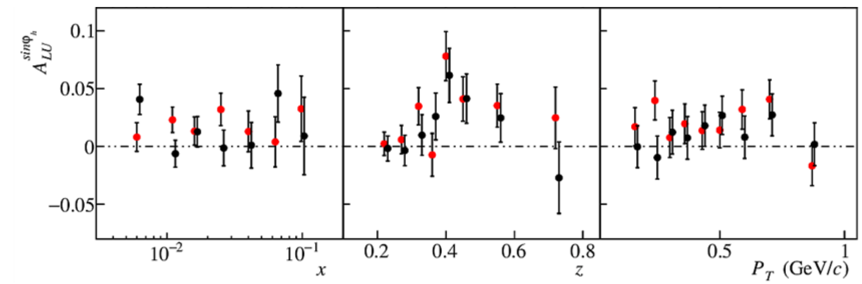

Comparison with deuteron results

Exclusive hadrons discarded / subtracted

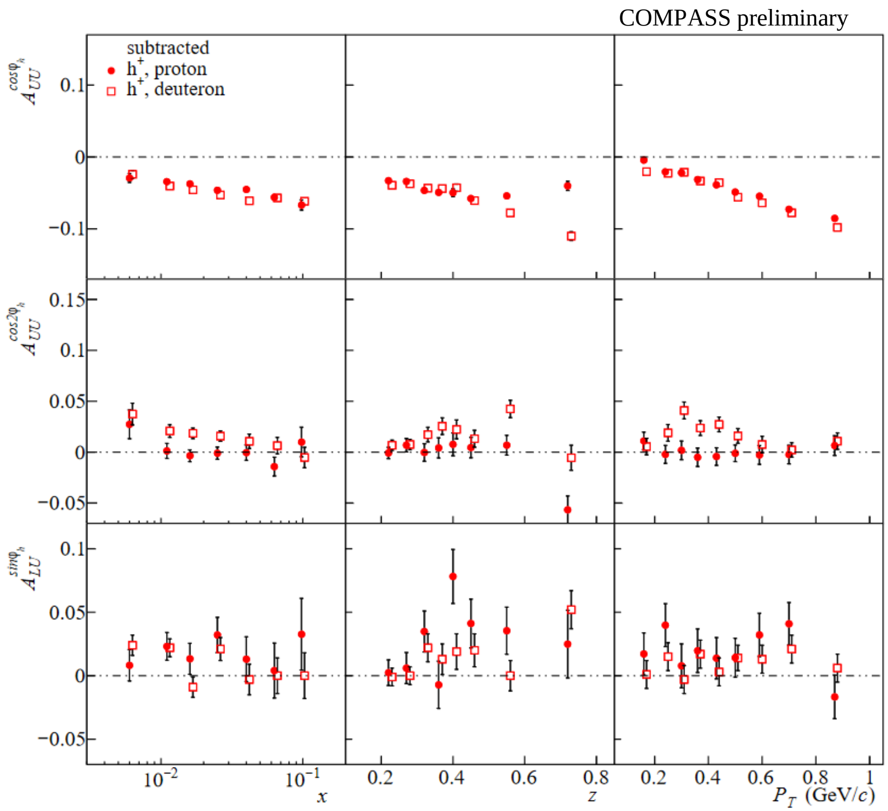

*Exclusive hadrons **not** discarded / subtracted*

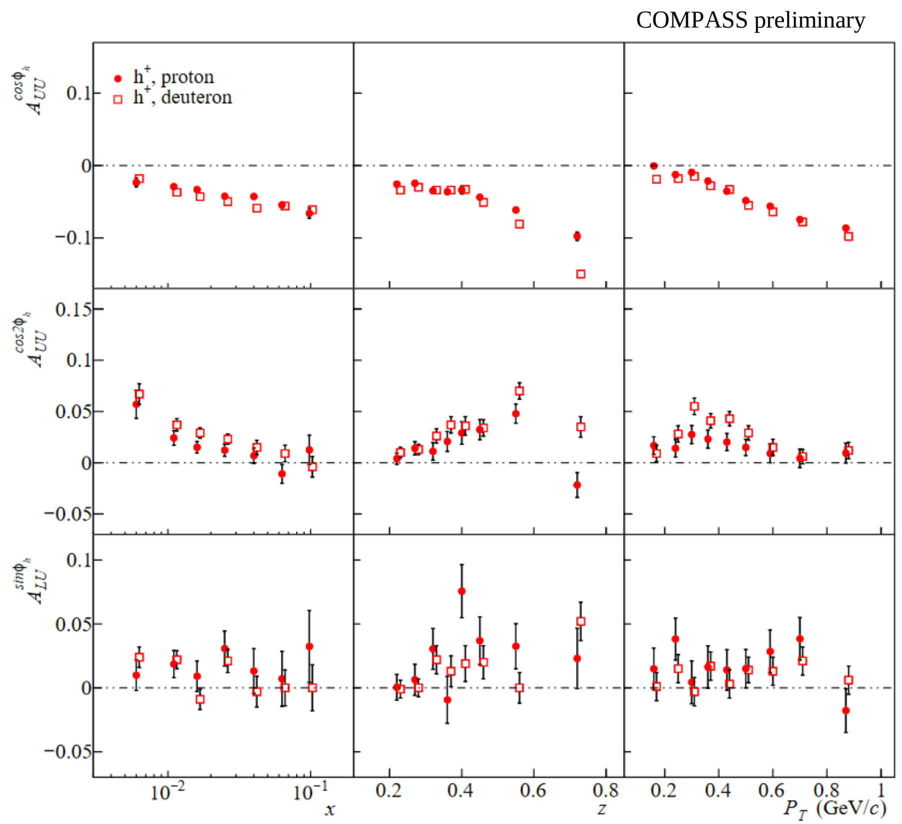

Difference visible also *before* the DVM subtraction / correction

Comparison with deuteron results

Current results (full points) compared to published results on deuteron **[COMPASS, NPB 956 (2020) 115039].**

Proton and deuteron results are in good agreement, as observed in other experiments (HERMES).

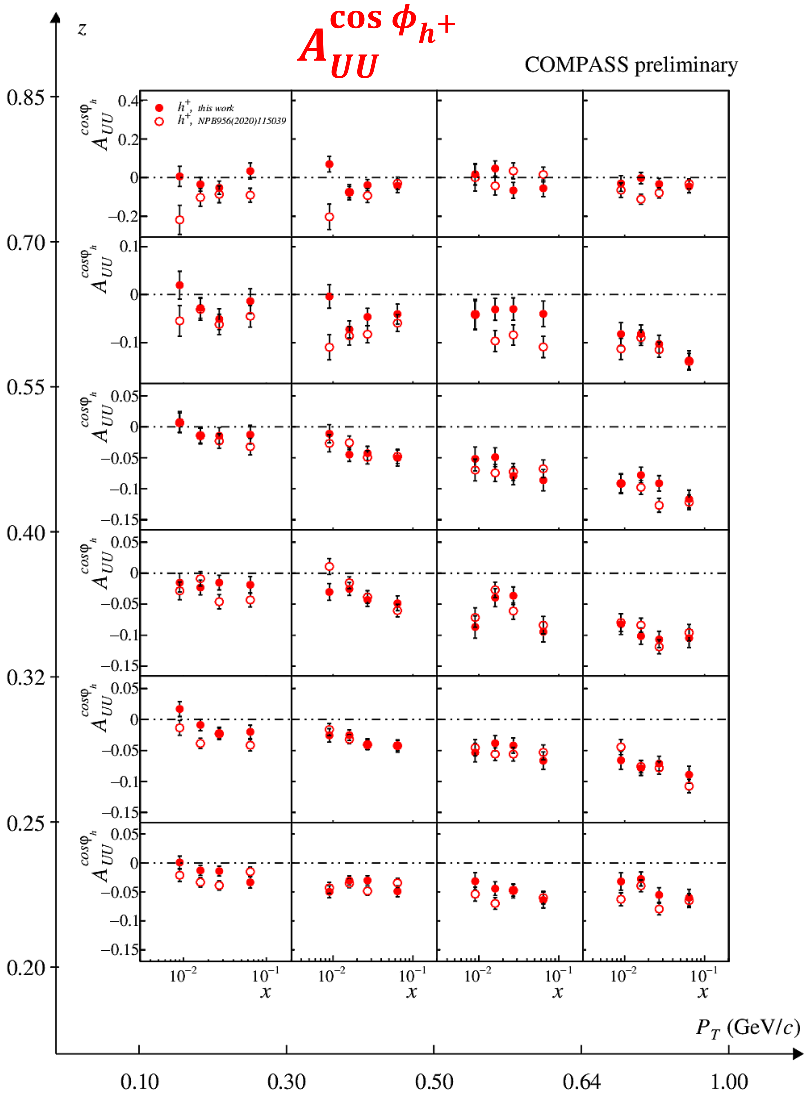

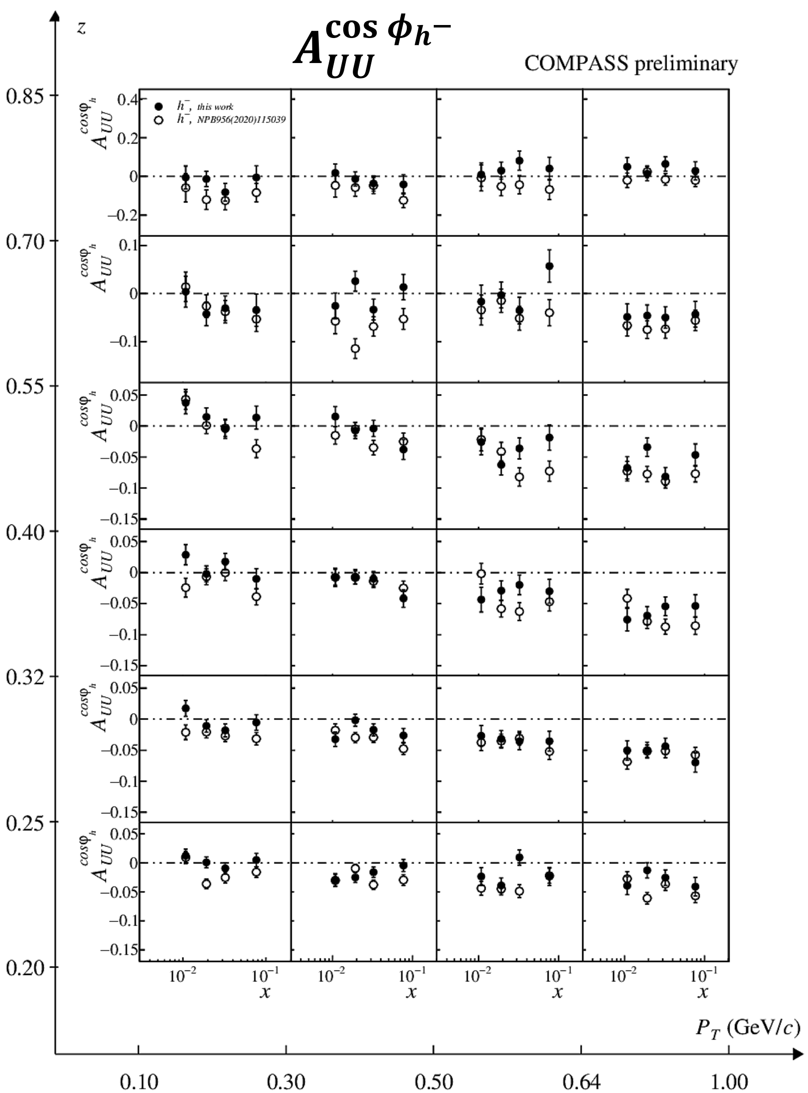

Comparison with deuteron results

Current results (full points) compared to published results on deuteron **[COMPASS, NPB 956 (2020) 115039].**

Proton and deuteron results are in good agreement, as observed in other experiments (HERMES).

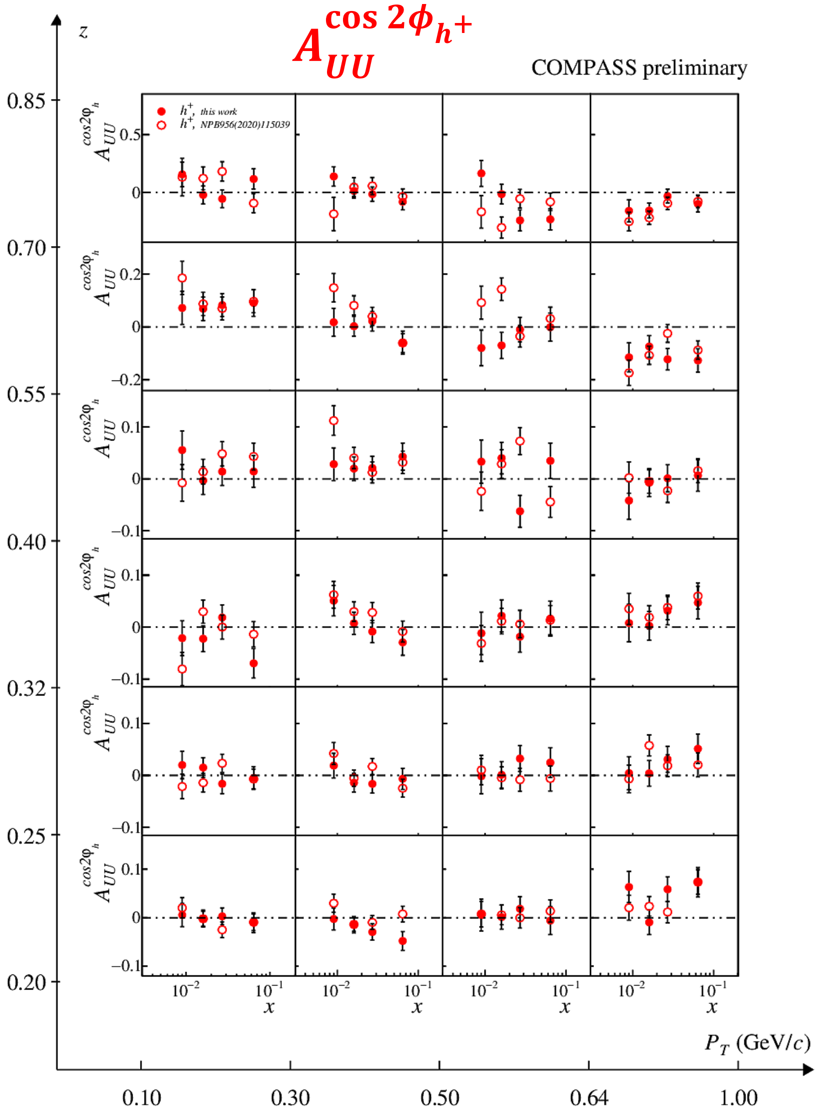

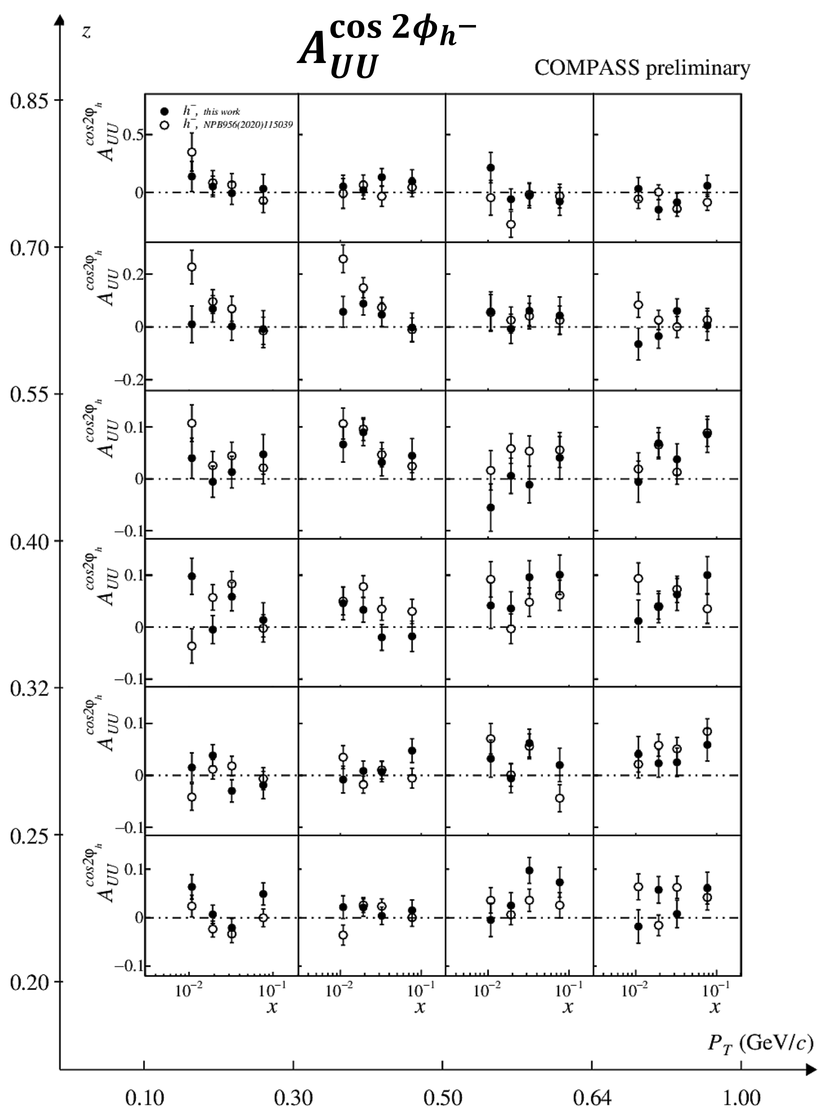

Acceptance

$$c_{acc}(P_T^2) = \frac{N_h^{rec}(P_T^{rec\,2})}{N_h^{gen}(P_T^{gen\,2})}$$

The acceptance is shown here in the first z bin, for positive and negative hadrons.
A flat plateau at values larger than 50% and, in some bins, a decrease at large P_T^2.

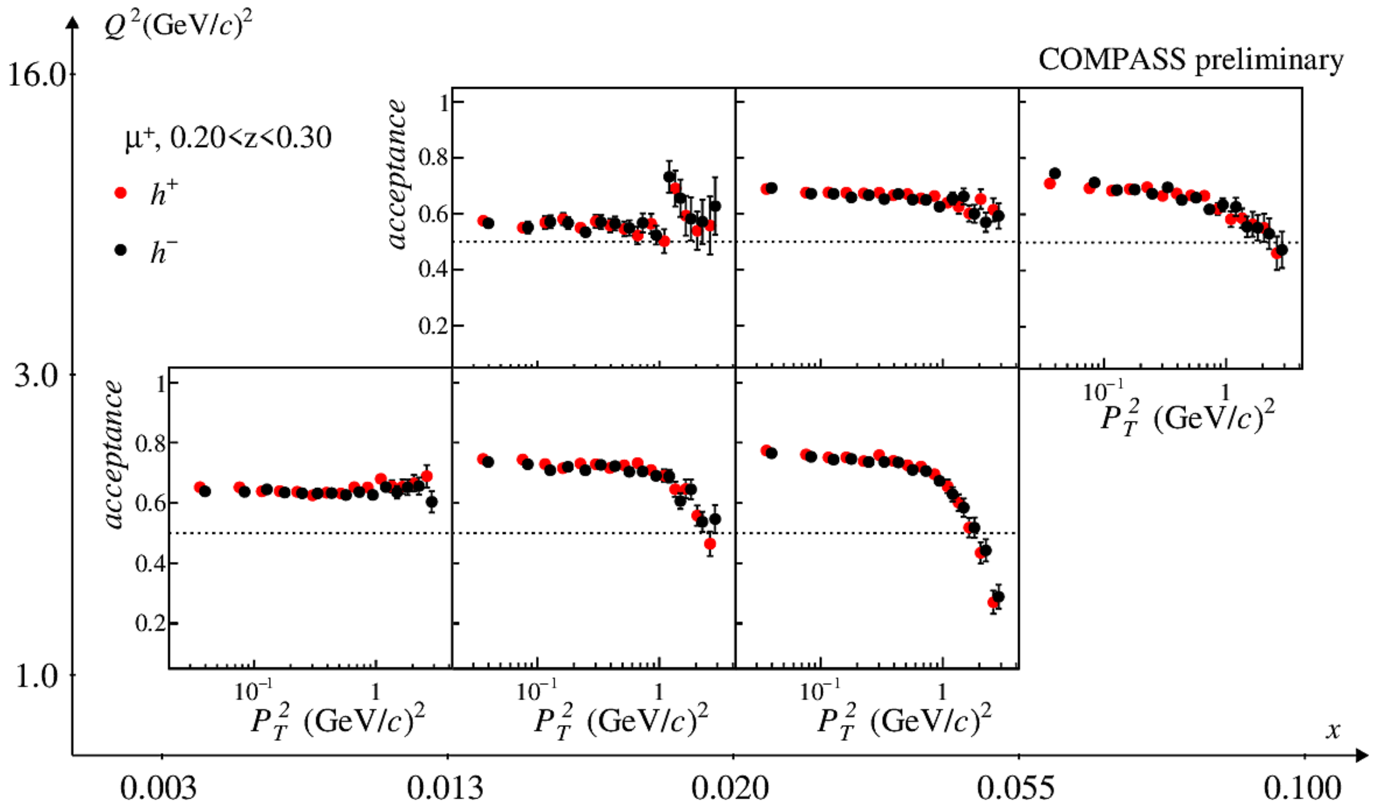

Comparison with deuteron results

The new results are compared to published results on a deuteron target **[COMPASS, PRD97(2018) 032006]**

The old results have been renormalized over the first point and averaged over x and Q^2 in order to match the current binning, while the z and P_T^2 binning has not been modified.

The agreement between new proton results and old deuteron ones is given in the plot on the right

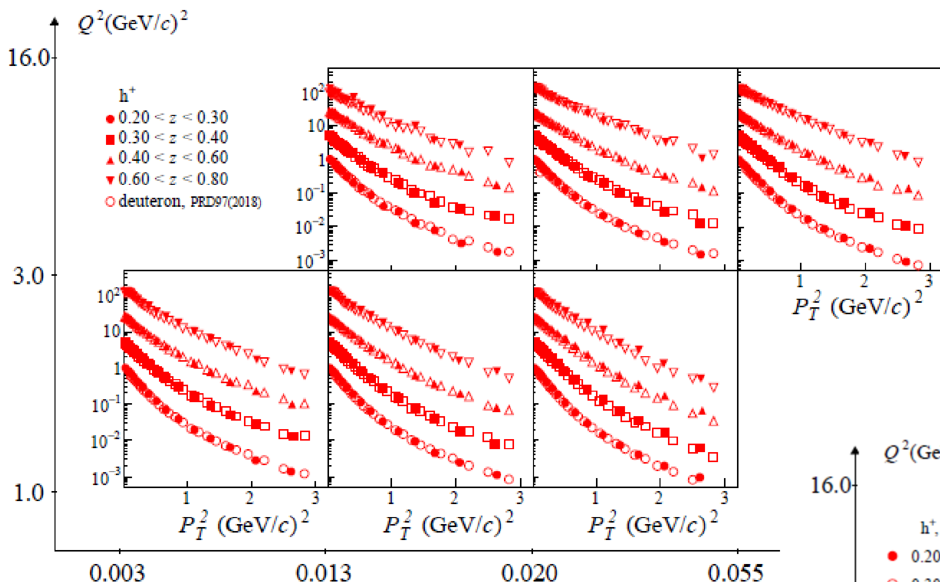

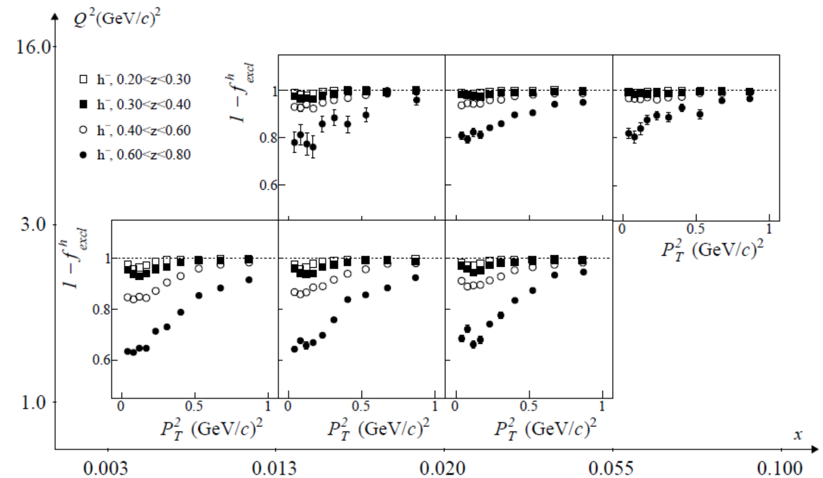

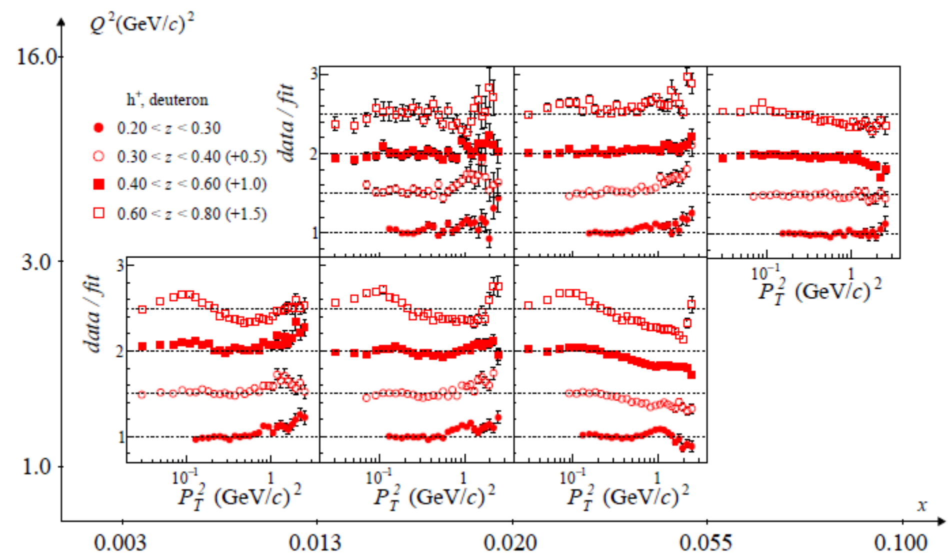

Exclusive ρ^0 Spin Density Matrix Elements

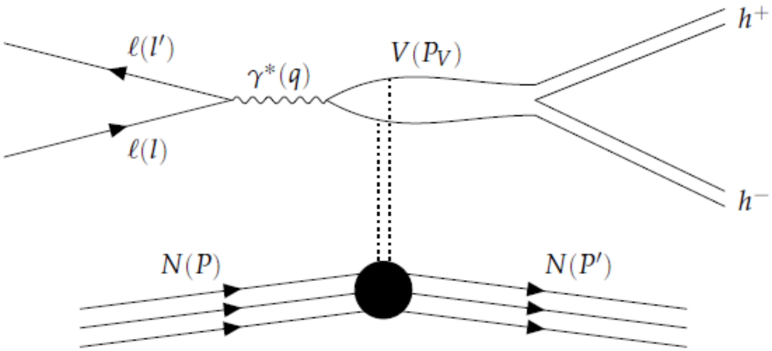

The diffractive production of a vector meson V and its decay into a hadron pair

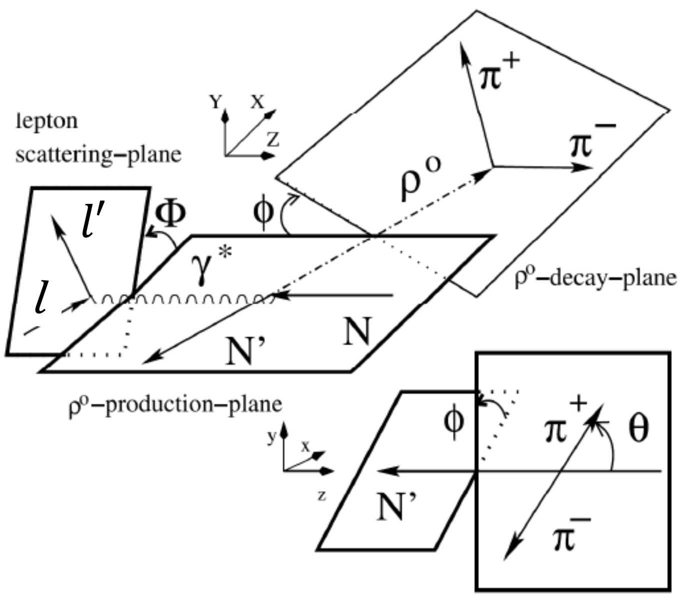

$$
\begin{aligned}
W^U(\cos\theta,\Phi,\phi) = \frac{3}{8\pi^2}\Bigg[& \frac{1}{2}\left(1-r^{04}_{00}\right)+\frac{1}{2}\left(3r^{04}_{00}-1\right)\cos^2\theta-\sqrt{2}\mathrm{Re}\left\{r^{04}_{10}\right\}\sin 2\theta\cos\phi-r^{04}_{1-1}\sin^2\theta\cos 2\phi \\
& -\epsilon\cos 2\Phi\left(r^{1}_{11}\sin^2\theta+r^{1}_{00}\cos^2\theta-\sqrt{2}\mathrm{Re}\left\{r^{1}_{10}\right\}\sin^2\theta\cos\phi-r^{1}_{1-1}\sin^2\theta\cos 2\phi\right) \\
& -\epsilon\sin 2\Phi\left(\sqrt{2}\mathrm{Im}\left\{r^{2}_{10}\right\}\sin 2\theta\sin\phi+\mathrm{Im}\left\{r^{2}_{1-1}\right\}\sin^2\theta\sin 2\phi\right) \\
& +\sqrt{2\epsilon\left(1+\epsilon\right)}\cos\Phi\left(r^{5}_{11}\sin^2\theta+r^{5}_{00}\cos^2\theta-\sqrt{2}\mathrm{Re}\left\{r^{5}_{10}\right\}\sin 2\theta\cos\phi-r^{5}_{1-1}\sin^2\theta\cos 2\phi\right) \\
& +\sqrt{2\epsilon\left(1+\epsilon\right)}\sin\Phi\left(\sqrt{2}\mathrm{Im}\left\{r^{6}_{10}\right\}\sin 2\theta\sin\phi+\mathrm{Im}\left\{r^{6}_{1-1}\right\}\sin^2\theta\sin 2\phi\right)\Bigg]
\end{aligned}
$$

$$
\begin{aligned}
W^L(\cos\theta,\Phi,\phi) = \frac{3}{8\pi^2}\Bigg[& \sqrt{1-\epsilon^2}\left(\sqrt{2}\mathrm{Im}\left\{r^{3}_{10}\right\}\sin 2\theta\sin\phi+\mathrm{Im}\left\{r^{3}_{1-1}\right\}\sin^2\theta\sin 2\phi\right) \\
& +\sqrt{2\epsilon\left(1-\epsilon\right)}\cos\Phi\left(\sqrt{2}\mathrm{Im}\left\{r^{7}_{10}\right\}\sin 2\theta\sin\phi+\mathrm{Im}\left\{r^{7}_{1-1}\right\}\sin^2\theta\sin 2\phi\right) \\
& +\sqrt{2\epsilon\left(1-\epsilon\right)}\sin\Phi\left(r^{8}_{11}\sin^2\theta+r^{8}_{00}\cos^2\theta-\sqrt{2}\mathrm{Re}\left\{r^{8}_{10}\right\}\sin 2\theta\cos\phi-r^{8}_{1-1}\sin^2\theta\cos 2\phi\right)\Bigg]
\end{aligned}
$$

Exclusive ρ^0 Spin Density Matrix Elements

UML fit of the observed pion distributions, correcting for the apparatus acceptance, in three steps:

- SDMEs with no background correction
- SIDIS background fraction estimation and background SDMEs
- SDMEs with SIDIS background correction

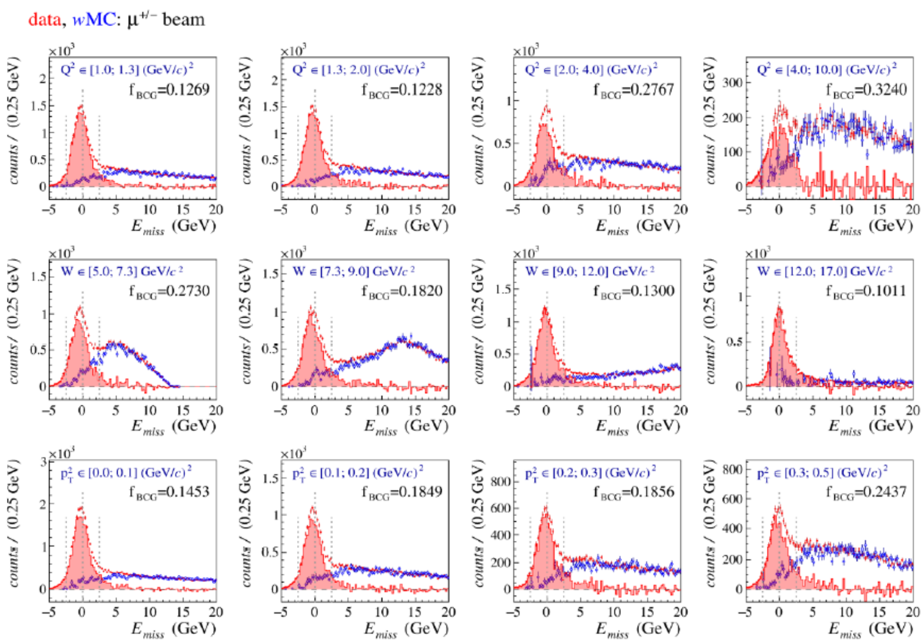

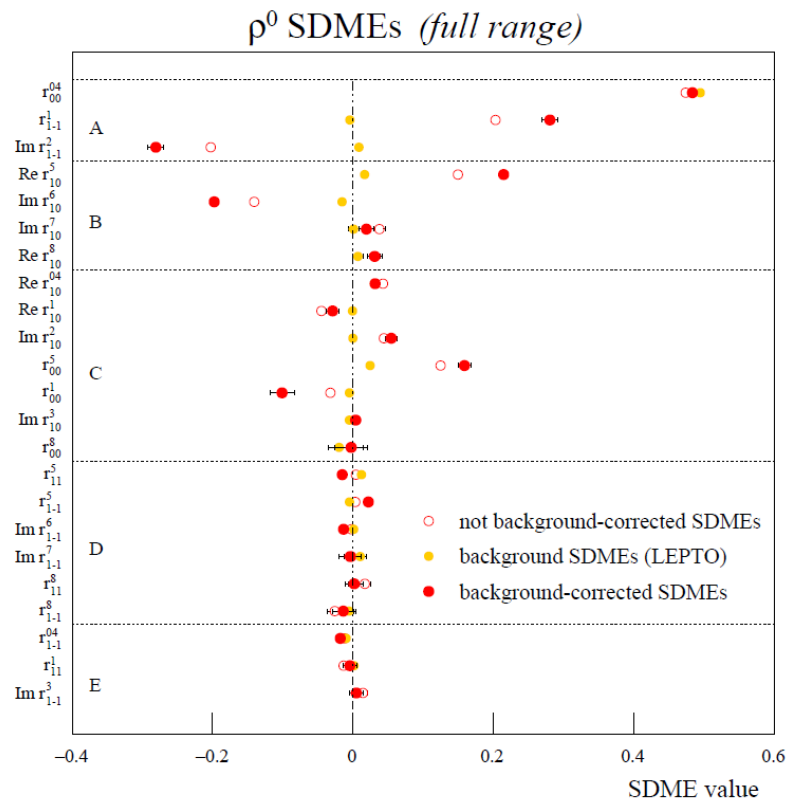

Exclusive ρ^0 Spin Density Matrix Elements